SLAC-PUB-2132
June 1978
(T/E)

An Experimental Summary of the XIII Rencontre de Moriond*

Martin L. Perl
Stanford Linear Accelerator Center
Stanford, California 94301

Abstract

This is the written version of a summary talk on some of the experimental results presented at the XIII Rencontre de Moriond. Results are reviewed in the following areas: (a) studies of the quark-parton model, Bjorken scaling, and quark fragmentation using virtual photons, neutrinos, and e^+-e^- annihilation; (b) properties of the τ lepton, D charmed meson, and F charmed meson as measured in e^+-e^- annihilation; (c) production of charmed particles by photons, neutrinos, and hadrons, including the CERN beam dump experiments; and (d) ongoing searches for new particles.

(Presented at the 13th Recontre de Moriond—Session I; High Energy Leptonic Interactions, Session II; High Energy Hadronic Interactions, Les Arcs (Savoie), France March 12-24, 1978.)

* Work supported by the Department of Energy.

TABLE OF CONTENTS

1. INTRODUCTION

At this XIIIth Rencontre de Moriond a tremendous amount of experimental and theoretical information had been presented — some new and some in the form of review. It is not possible in a summary talk to cover all this material or to do justice to the many fine presentations. Therefore, I have adopted two limits on the material I will discuss. First, I will not review any theory; a general theoretical talk has been presented by Cabibbo[1], and, in any case, I am not competent to report on much of the theoretical work presented here. Second, I have limited this talk to those experimental topics which seemed most in need of review either because a large amount of new material was presented; or because it seemed worthwhile to compare results from different areas such as neutrino physics and virtual photon physics; or because the topic still seemed to have a large amount of experimental uncertainty and incoherence. I hope that my use of this last criterion has not introduced too much incoherence into this talk.

2. VIRTUAL PHOTONS, NEUTRINOS, AND THE QUARK-PARTON MODEL

2A. The Interaction of Spacelike Virtual Photons with Quarks

As we all know, deep inelastic electroproduction or muoproduction occurs in the quark-parton model, Fig. 1a, through the fundamental reaction[2),3)]

$$\gamma_{\text{virtual, spacelike}} + \text{quark} \rightarrow \text{quark} \tag{1}$$

We also know that this reaction is described by three structure functions

$$F_1^{em}(\nu,q^2),\ F_2^{em}(\nu,q^2),\ F_3^{em}(\nu,q^2) \tag{2}$$

where ν is the energy of the virtual photon in the laboratory system and q^2 is the square of its four-momentum. Bjorken scaling says that these F's for sufficiently large ν and $|q^2|$ should only be a function of a single variable called x or ω where

$$x = \frac{1}{\omega} = \frac{Q^2}{2M\nu} \tag{3}$$

with $Q^2 = |q^2|$ and M the proton mass. Electroproduction experiments at SLAC by SLAC and MIT groups first established the validity of Bjorken scaling for F_1^{em} and F_2^{em} when $Q^2 \gtrsim 1(\text{GeV/c})^2$. ($F_3^{em}$ can only be determined through the inelastic scattering of polarized leptons on polarized nucleons; and this has only been accomplished recently.[4)]) The acceptance of the validity of

Bjorken scaling for Reaction 1 has meant that we could simply regard Reaction 1 as the absorption of a virtual photon by a free quark — the quark being simply a charged point particle.

While this picture has proved to be very useful, we must now accept the fact that violations of Bjorken scaling have been found experimentally using electrons at SLAC[5] and muons at Fermilab.[6),7] The explanation for these violations is simply that the quark is not free; rather the quark interacts with other quarks and with gluons in the nucleon. We should not be surprised at this; indeed, we should be more surprised the Bjorken scaling and the free quark concept work as well as they do. The concept of asymptotic freedom and the theory of quantum chromodynamics provide a framework for understanding why Bjorken scaling works and for studying the violations of Bjorken scaling. These ideas have been reviewed by G. Alterelli[8] at this conference; and, as I stated in the Introduction, I will not discuss these theoretical ideas again here. However, at the end of the next section I will use a bit of parameterization from quantum chromodynamics, the Λ parameter, to compare neutrino data with muoproduction data.

The most recent measurements of Bjorken scaling violations in muoproduction, TABLE I, were presented by T. Quirk[9] and W. Chen[10]. Figure 2 shows $F_2^{em}(x)$ for the 147 GeV μ-p data[9] compared to a fit to the lower energy electron data. We note that over this ν range it is a useful approximation to think of $F_2(x)$ at fixed Q^2 as independent of ν. The curves from Fig. 2 are superimposed in Fig. 3. We see that for

$$x \lesssim 0.25 \quad F_2(x) \text{ increases as } Q^2 \text{ increases} \tag{4a}$$

$$x \gtrsim 0.25 \quad F_2(x) \text{ decreases as } Q^2 \text{ increases} \tag{4b}$$

This observation has been made quantitative by Perkins et al[11] who used the scaling violation parameterization

$$F_2(x,Q^2) = F_2(x,Q_o^2) \left[\frac{Q^2}{Q_o^2}\right]^b \tag{5}$$

Fig. 4 prepared by T. Quirk[9] shows that the simple rule[11]

$$b = 0.25 - x \tag{6}$$

is a useful approximation. There are no corresponding measurements on $F_1(x)$ violations of scaling because $F_1(x)$ is multiplied by $\sin^2 \theta/2$ (θ is the electron scattering angle in the laboratory) and is therefore very difficult to measure.

TABLE I

Muoproduction Experiments

Speaker	T. Quirk	W. Chen	W. Chen
Experimental parameters	μ-p, μ-D E_μ = 96,147 GeV $0.3 \lesssim Q^2 \lesssim 50.$ $(GeV/c)^2$	μ-Fe E_μ = 56,150 GeV $1 \lesssim Q^2 \lesssim 40$ $(GeV/c)^2$	μ-Fe E_μ = 270 GeV $5 \lesssim Q^2 \lesssim 150$ $(GeV/c)^2$
Reference	6, 9	7	10
Groups	Chicago, Harvard, Illinois, Oxford	Cornell, LBL, Mich. State, UCSD	Mich. State, Fermilab
Laboratory	Fermilab	Fermilab	Fermilab

Chen[10] presented very large Q^2 muoproduction data, Fig. 5, using an iron target. The curves are Chen's fits[10] to the SLAC-MIT data[5] at lower ν and Q^2 extrapolated to higher Q^2. The $5 < Q^2 < 15$ $(GeV/c)^2$ data is in fairly good agreement with the corresponding μ-p data, Fig. 2. And, as Q^2 increases, F_2 also appears to continue to increase for $x \lesssim .2$. This is a further illustration of Eq. 4a. Chen[10] also presented his data for fixed intervals in ω, Fig. 6. When $\omega>5$ (that is $x < .2$) the increase of F_2 with Q^2 is clear. The $3 < \omega < 5$ plots show a non-monatonic behavior that can be interpreted, as pointed out by Chen, as an indication of a threshold for some new particle production at a total hadronic energy of about 10 GeV. However, this phenomenon and its threshold interpretation are probably best regarded as a stimulus for further measurements of F_2 in this high Q^2 range.

Incidently, a comprehensive review of electroproduction and muoproduction has been given recently by Hand.[3]

2B. The Interaction of Neutrinos with Quarks

Figure 1b reminds us that the fundamental reaction

$$W + \text{quark} \rightarrow \text{quark} \qquad (7)$$

where W is the intermediate boson which carries the weak interactions, is analogous to Reaction 1. If we accept the unification of weak interactions and electromagnetic interactions, then Reaction 7 should also show (a) approximate Bjorken scaling, and (b) violations of that scaling analogous to those

exhibited by Reaction 1. Point (a) is now well extablished[12),13),14)] for both neutrinos and anti-neutrinos, and so we can immediately turn to point (b) — the violations of Bjorken scaling.

B. Tallini[14)] presented measurements, Fig. 7, of the scaling violation of F_2^{ν} from BEBC and Gargamelle data (TABLE II). The dashed lines are fits to lower energy

TABLE II

Neutrino experiments on Bjorken scaling violations

Speaker	B. Tallini	A. Savoy-Navarro
Experimental parameters	ν and $\bar{\nu}$ in Gargamelle with $2 < E_\nu < 12$ GeV ν and $\bar{\nu}$ in BEBC with $20 < E_\nu < 200$ GeV	ν and $\bar{\nu}$ in CDHS counter, drift chamber experiment with $30 < E_\nu < 200$ GeV
Reference	14	13
Laboratory	CERN	CERN

electroproduction data; they show that very similar scaling violations are observed in F_2^{ν} and F_2^{em}. The difference between ν and $\bar{\nu}$ deep inelastic scattering yields directly F_3^{ν}; and, as shown in Fig. 8, xF_3^{ν} shows violations similar to F_2^{ν}. (We use xF_3^{ν} because in the simple quark-parton model $|xF_3^{\nu}| = F_2^{\nu}$.)

The CDHS data as presented by A. Savoy-Navarro[13)] is not yet in a form for direct comparisons with Fig. 7. However, Fig. 9 shows that there are scaling violations in $F_2(x)$ in quantitative agreement with Fig. 7 and Eq. 4. This follows from Fig. 10 which shows that in the CDHS data $\langle Q^2/E_{\nu,\bar{\nu}}\rangle$ is constant. Hence in Fig. 9 the larger E_ν curve is on the average a larger Q^2 curve. Incidently, Fig. 10 shows that the change in $\langle Q^2/E_{\nu,\bar{\nu}}\rangle$ which is apparent in the combined GGM-BEBC data (and which is also an indication[12)] of a scaling violation) is not seen in the exclusively high energy CDHS data. A similar remark applies to Fig. 11.

It has become conventional[15)] to describe scaling violations in quantum chromodynamics through a scale parameter Λ (GeV/c) which enters the theory through the function $\ln(Q^2/\Lambda^2)$. For example: Buras and Gaemers[15)] replace the usual expressions

$$F_2(x) = \sum_i x^{a_i} (1 - x)^{b_i}; \; a_i, \; b_i \text{ constants}, \tag{8a}$$

which obey Bjorken scaling, by

$$F_2(x, Q^2) = \sum_i x^{a_i(\bar{s})} (1-x)^{b_i(\bar{s})} \tag{8b}$$

In this latter expression

$$\bar{s} = \ln\left[\frac{\ln \frac{Q^2}{\Lambda^2}}{\ln \frac{Q_o^2}{\Lambda^2}}\right] \tag{8c}$$

Electroproduction and muoproduction data gives values of Λ in the range of 0.3 to 0.66 GeV/c depending on the fitting method[15]. Tallini[14] gives $\Lambda = 0.75 \pm 0.1$ GeV/c for the neutrino data. It is too soon to say whether this difference has any significance because: (a) different ranges of ν and Q^2 occur in the different experiment, (b) the various experiments may have different systematic errors, and (c) different fitting methods have been used. However, as virtual photon and neutrino experiments improve in statistics, it will be interesting to test just how precisely the scaling violations agree.

2C. The Interaction of Timelike Virtual Photons with Quarks

The fundamental reaction, Fig. 12, is

$$\gamma_{\text{virtual, timelike}} \rightarrow \text{quark} + \text{anti-quark} \tag{9}$$

and this reaction is most easily studied through electron-positron annihilation,

$$e^+ + e^- \rightarrow \text{hadrons} \tag{10}$$

The analogy to Bjorken scaling in Reaction 9 is the statement[16] that

$$R = \sigma_{e^+e^- \rightarrow \text{hadrons}} \; / \; \sigma_{e^+e^- \rightarrow \mu^+\mu^-} = \text{constant} \tag{11}$$

Of course this can only be tested in an energy region where there are no thresholds for new particle production. Such a region appears to be $5 \lesssim E_{cm} \lesssim 9$ GeV; just below 5 GeV there are presumably charmed baryon thresholds, and above 9 GeV thresholds associated with the upsilon will occur. G. Wolf[17] presented new measurements of $\sigma_{e^+e^- \rightarrow \text{hadrons}}$ from the DASP collaboration Fig. 13; and Fig. 14 is a recent SLAC-LBL compilation[18] of $\sigma_{e^+e^- \rightarrow \text{hadrons}}$. Above 5 GeV $R_{exp} = 5.3$ to 5.5 and in the SLAC-LBL data is a constant. Thus we do see Bjorken scaling. However, the magnitude of R_{exp}

is higher than the simple quark model prediction[19] of R = 4.33, which includes the u, d, s, and c quarks, and the τ lepton. Thus

$$R_{exp} - R_{theor} \sim 1 \text{ for } E_{cm} > 5 \text{ GeV} \tag{12}$$

We do not know the reason for this discrepancy.

2D. Quark Fragmentation

Here we are concerned with comparing how

$$\text{quark} \rightarrow \text{hadrons} \tag{13}$$

after the quark is excited or created in Reactions 1, 7, or 9. I shall limit my discussion here to the single hadron inclusive distribution, Eq. 14, and I shall neglect the mass

$$\text{quark} \rightarrow h + \text{other hadrons} \tag{14}$$

of the produced hadron (h). Then in all three of the reactions there is a maximum momentum p_{max} which can be given to h; and we define the longitudinal variable

$$z = p_{longitudinal}/p_{max} \tag{15}$$

and the transverse momentum p_T; relative to the direction of motion of the fragmenting quark.

As has been demonstrated beautifully by G. Hanson[18], the proper determination of z in e^+e^- annihilation (Eq. 9) requires the finding of a jet axis; and then the calculation of z and p_T relative to that axis. These variables are used in Fig. 15, prepared by T. Quirk[9], in which e^+e^- annihilation is compared with μ-p deep inelastic scattering (TABLE I). This is an absolute comparison. We see the pleasing result that the distribution functions $(z/\pi\sigma)(d\sigma/dz)$ are the same except in the lowest z bin.

Y. Sacquin[20] used ν and $\bar{\nu}$ data with $E_\nu > 100$ GeV from BEBC to show, Fig. 16, that the z distributions for ν and $\bar{\nu}$ reactions are quite similar[22] to those for electroproduction[21] and e^+e^- annihilation.[23] (The e^+e^- data here is not relative to the jet axis.)

Turning to the p_T distributions we first look at some interesting new results in the ν and $\bar{\nu}$ data presented by Y. Sacquin[20], Fig. 17. Here as Q^2 increases, $\langle p_T \rangle$ at fixed z increases. This is the first demonstration, to my knowledge[24], of an effect of Q^2 on $\langle p_T \rangle$ in inclusive hadron production properties in deep inelastic lepton scattering.

Finally, in Fig. 18 we compare $\langle p_T \rangle$ for e^+e^- annihilation[18], muoproduction[9], and ν deep inelastic scattering. For the latter we use the $5 < Q^2 < 10$ $(GeV/c)^2$ data of Sacquin[20]. We see quite similar $\langle p_T \rangle$ values.

2E. Conclusions for Section 2

(a) Deep inelastic electron, muon and neutrino scattering all show similar violations of Bjorken scaling which qualitatively follow Eq. 4. For $Q^2 > 20$ $(GeV/c)^2$ and $\omega \sim 4$ there may be more complicated behavior versus Q^2.

(b) In e^+e^- annihilation above $E_{cm} = 5$ GeV, R shows Bjorken scaling but simple theory does not explain the high value of R.

(c) Quarks change into hadrons in the same way whether produced by deep inelastic lepton scattering or in e^+e^- annihilation; as we expect from the quark model. An interesting effect of Q^2 on $\langle p_T \rangle$ has been seen in ν experiments.

3. PROPERTIES OF NEW PARTICLES FROM e^+e^- ANNIHILATION

This discussion of the τ lepton, D charmed meson, F charmed meson, and charmed baryons is based on the electron-positron annihilation experiments listed in TABLE III.

TABLE III

e^+e^- Experiments Presented at this Conference

Speaker	Apparatus or Group Name	Storage Ring
J. Bürger	PLUTO	DORIS
G. Grindhammer	DASP	DORIS
G. Wolf	DASP	DORIS
G. Hanson	SLAC-LBL Mark I	SPEAR
M. Perl	SLAC-LBL Mark I	SPEAR
	LBL-SLAC Lead Glass Wall Detector	
A. Diament-Berger	DELCO	SPEAR

3A. Properties of the τ Lepton

All the known properties of the τ, (TABLE IV) are consistent with it being a lepton.

TABLE IV

Properties of the τ lepton. Some of these properties were presented or published after this conference. Decay modes are always written for the τ^- to simplify the notation.

General Property	Value or Specific Property or Comment	Reference
τ Mass (GeV/c^2)	1807 ± 20 $1782 \begin{smallmatrix}+2\\-7\end{smallmatrix}$	(DASP) 17, 28 (DELCO), 27, 29
ν_τ Mass	<250 MeV/c^2 with 90% confidence	(DELCO) 27
τ-ν_τ Coupling	V+A excluded V+A excluded, Michel parameter $\rho = 0.73 \pm 0.15$	(SLAC-LBL) 30 (DELCO) 27
Lepton Type	Sequential or τ^- has lepton number of e^-	30, 31, 32, 33, 34, 35
Lifetime	$<10^{-11}$ sec. with 95% confidence $<4 \times 10^{-12}$ sec. with 95% confidence	(SLAC-LBL) 30 (PLUTO) 36
Leptonic Branching Ratio	$B(\tau^- \to \nu_\tau e^- \bar{\nu}_e) = B(\tau^- \to \nu_\tau \mu^- \bar{\nu}_\mu)$ to within 10 or 20% $B(\tau^- \to \nu_\tau e^- \bar{\nu}_e) = 18.2 \pm 2.8 \pm 1.4\%$ $B(\tau^- \to \nu_\tau e^- \bar{\nu}_e\ 1 = 18.6 \pm 1.0 \pm 2.8\%$ $B(\tau^- \to \nu_\tau e^- \bar{\nu}_e) = 16.3 \pm 1.0\%$	 (DASP) 17, 28 (SLAC-LBL) 30,37 (DELCO) 27, 29
$\tau^- \to \nu_\tau + \pi^-$	$B(\tau^- \to \nu_\tau \pi^-) = 8.3 \pm 3\%$ General evidence for this decay mode has been found by G. Hanson. This mode has not been seen by a small statistics DASP search	(DELCO) 29 (SLAC-LBL) 38 (DASP) 17
Other Hadronic Decay Modes	$B(\tau^- \to \nu_\tau \rho^-) = 24 \pm 9\%$ $B(\tau^- \to \nu_\tau \pi^- \pi^+ \pi^-) = 5 \pm 1.5\%$ with evidence for A_1 $B(\tau^- \to \nu_\tau \pi^- \pi^+ \pi^-) = 6 \pm 4.5\%$; this data is consistent with A_1 but does not require it. $B(\tau^- \to \nu_\tau \pi^- \pi^+ \pi^- \pi^o) = 10 \pm 7\%$	(DASP) 17, 28 (PLUTO) 25, 39 (SLAC-LBL) 40 (SLAC-LBL) 40
Other Decay Modes	No other decay modes such as $\tau^- \to e^- \gamma, \tau^- \to \mu^- \gamma$ $\tau^- \to \nu_\tau e^- e^+ e^-$ have been seen	For a summary see Ref. 30
Spin	The energy dependence of the production cross section is consistent with spin = ½ and appears to be inconsistent with other spins; although more quantitative work needs to be done here	41

3B. D Charmed Mesons

The hadronic decay modes

$$D^o \to K^-\pi^+, \bar{K}^o\pi^+\pi^-, K^-\pi^+\pi^o, K^-\pi^+\pi^-\pi^+$$
$$D^+ \to \bar{K}^o\pi^+, K^-\pi^+\pi^+ \qquad (16)$$

have been seen. A thorough review has been given by Feldman[42] and we only note here that all the properties of these hadronic decays are consistent with the conventional theory of weak interactions and charmed quarks[19].

The semi-leptonic decay modes, Eq. 17, branching ratios

$$D^o \to e^+ + \nu_e + (\text{hadrons})^-$$
$$D^+ \to e^+ + \nu_e + (\text{hadrons})^o \ ; \qquad (17)$$

and more general

$$\text{charm particle} \to e + \nu_e + \text{hadron} \qquad (18)$$

branching ratios are given in TABLE V.

TABLE V

Energy Range	Branching Ratio	Reference
At $\psi(3772)$	$B(D \to e + X) = 7.2 \pm 2.8\%$ averaged over D^o and $D^\pm$	(LBL-SLAC)43
$3.9 \leq E_{cm} \leq 7.8$ GeV	$B(\text{charm} \to e + X) = 8.2 \pm 1.9\%$	(LBL-SLAC)43
$4 \leq E_{cm} \leq 5.2$ GeV	$B(\text{charm} \to e + X) = 7.2 \pm 2.0\%$	(DASP)17
At $\psi(3772)$	$B(D \to e + X) = 11 \pm 2\%$ averaged over D^o and $D^\pm$	(DELCO)27, 44

The $e^\pm$ momentum spectrum for Eq. 17 is given in Fig. 19. This is DELCO data[27] obtained at the $\psi(3772)$ and averaged over D^o and $D^\pm$ decays. The spectrum is consistent with a mixture of $D \to e\nu K$ and $D \to e\nu K^*(890)$ decay modes with V-A coupling.

3C. F Charmed Mesons

Information on the F meson is still scanty. DASP[17), 45] has previously reported seeing the

$$F^\pm \to \eta + \pi^\pm \qquad (19)$$

decay mode at $E_{cm} = 4.4$ GeV. This data yields masses of

$$M_F = 2030 \pm 60 \text{ MeV/c}^2, \ M_{F^*} = 2140 \pm 60 \text{ MeV/c}^2 \ ; \qquad (20)$$

and at this conference G. Wolf[17] reported an inclusive η peak at E_{cm} = 4.16 GeV, Fig. 20. This appears to be evidence for

$$e^+ + e^- \rightarrow F + \bar{F} \tag{21}$$

at 4.16 GeV since the η peak is not seen at 4.03 GeV, Fig. 21.

D. Lüke[46] has discussed searches for the F using all charged particle decay modes such as

$$F^{\pm} \rightarrow K^+ + K^- + \pi^{\pm} \tag{22}$$

3D. Charmed Baryons

No direct evidence for the production of charmed baryons in e^+e^- annihilation has been found. Figure 22 from the SLAC-LBL collaboration[47] presents indirect evidence for a threshold for charmed baryon production at an E_{cm} of roughly 4.5 GeV.

3E. Conclusions for Section 3

(a) All measured properties of the τ are consistent with it being a lepton and no other hypothesis as to the nature of the τ fits the data.

(b) The known decay modes of the D meson are consistent with conventional theory.

(c) The branching ratio for charmed particle → e + X is in the 7 to 11% range, averaged over the production cross section for charmed particles in e^+e^- annihilation.

(d) Much more work remains to be done on F production in e^+e^- annihilation; and charmed baryons have not yet been found directly in e^+e^- annihilation.

4. PRODUCTION OF CHARMED PARTICLES BY PHOTONS, HADRONS, AND NEUTRINOS

4A. Photoproduction of Charmed Particles

F. Richard[48] reported that 8 events of the form

$$\gamma + p \rightarrow D + X \qquad \text{(23)}$$
$$\hookrightarrow K^-\pi^+$$

have been found using the Omega Facility at CERN with $25 < E_\gamma < 72$ GeV. This corresponds to a production cross section for the D in the range of one to

several microbarns. This is a reasonable value because the total hadronic cross section is about 100 microbarns. This is the first report of photoproduction of charmed mesons.

4B. Direct Experiments on Hadroproduction of Charmed Particles

In this section we review experiments which have looked for hadronic production of charm by searching for

$$D \to K^{\pm} + \pi \tag{24}$$

$$\text{charm particle pair} \to e^{\pm} + \mu^{\mp} + X \tag{25}$$

$$\text{charm particle pair} \to \mu^{\pm} + \mu^{\mp} + X \tag{26}$$

$$\text{charm particle} \to \mu^{\pm} + X \tag{27}$$

TABLE VI gives published results on some experiments which have not found a charmed particle signal and so can only give upper limits. These upper bounds depend upon combining the acceptance of experiment with a model for the x and p_T distributions of charmed particles produced in hadronic interactions. This of course leads to an uncertainty in how to interpret these upper limits. I have not made a study of this problem; and so looking at TABLE VI I simply estimate that the cross section for the hadronic production of D^o mesons is less than several tens of μb in the energy range of the table. The cross sections for $D^o + D^{\pm}$ production could be twice as large; and the limit on the hadronic production of all types of charmed particles seems to be of the order of magnitude of 100 μb. The reader should make his or her own estimates.

This is now one experiment[49] which has finally detected charmed particle production by hadrons. This experiment carried out at Fermilab by a CIT-Stanford collaboration[49], used the apparatus in Fig. 23 with a 400 GeV proton beam. One part of the data collection consists of looking for events with a prompt, single muon. This data was corrected for feed-down from dimuon events and for contamination by muons from the decay of conventional particles—pions and kaons. The latter correction was made by varying the density of the target. The experimenters find a non-zero, prompt, single muon signal. If they assume the single muons come from the decay of a D meson produced with the distribution $dN/dx_F dp_T^2 = e^{-2.04 p_T}(1-|x_F|)^{4.67}$ and that the nuclear production cross sections is proportional to A then their preliminary result is

$$\sigma(\text{charm}) \sim 40\ \mu b \quad . \tag{28}$$

TABLE VI

Published limits in μb/nucleon for some searches for hadronic production of charmed particles. All limits assume that the nuclear production cross section is proportional to A

Experiment	Method	Limit and Comments	Reference
M.A. Abolins et al.	$n + Be \rightarrow D^o + \bar{X}$ $D^o \rightarrow K^\pm + \pi^\mp$ $<E_n>$=250 GeV	No signal found. A 4 s.d. effect would require $\sigma_{D^o}(x>0)$=14 μb/nucleon	Phys.Lett. 73B, 355 (1978)
W.R. Ditzler	$p + Be, CH_2, Pb \rightarrow$ $D^o + X$ $D^o \rightarrow K^\pm + \pi^\mp$ E_p = 400 GeV	No signal found. $d\sigma_{D^o}/dy(y_{cm}=-0.4)$ <23 μb/nucleons with 95% confidence.	Phys.Lett. 71B, 451 (1978)
J.C. Alder et al.	$p + p \rightarrow D^o + X$ $D^o \rightarrow K^\pm + \pi^\mp$ E_{cm} = 53 GeV	No signal found. σ_{D^o}<770 μb/nucleon with 95% confidence. σ was measured for .9<y<1.2 and a model used to obtain the total σ.	Phys.Lett. 66B, 401 (1977)
A.M. Johckheere et al.	$\pi^- + C,H_2 \rightarrow$ $\mu^+ + \mu^- + X$	No signal found. $\sigma_{D\bar{D}}$ < 10.4 μb/nucleon with 90% confidence. $D\bar{D}$ production assumed similar to ψ production to calculate acceptance.	Phys.Rev. D16, 2073 (1977)
D. Spelbring et al.	$n + Be \rightarrow \mu + D^o + X$ $D^o \rightarrow K^\pm + \pi^\mp$ $<E_n>$=300 GeV	σ_{DC} < 64 μb/nucleon with 95% confidence. Used e^{-5x} and $\exp(-1.5\ p_T^2)$ to calculate acceptance.	Phys.Rev. Lett. 40, 607 (1978)
R. Lipton et al.	$n + Be \rightarrow \mu^\pm + e^\mp + X$ $<E_n>$ = 300 GeV	$\sigma_{c\bar{c}}$ <34 μb/nucleon with 95% confidence.	Phys.Rev.Lett. 40, 608 (1978)
G. Coremans-Bertrand et al.	p + emulsion → two particles with visible decays. E_p=300 GeV	σ <1.5 μb/nucleon with 90% confidence. However if a D lifetime of 3×10^{-13} sec and $<E_D>$=20 GeV is assumed, the limit becomes 10 μb/nucleon. This assumes 100% scanning efficiency.	Phys.Lett. 65B, 480 (1976).

If other D production models are used or if an $A^{2/3}$ nucleon production cross section is used, then σ(charm) can be in the range of 20 to 80 μb. In comparing Eq. 28 with TABLE VI the reader should remember that Eq. 28 includes $D^{o}\bar{D}^{o}$ pairs, $D^{\pm}D$ pairs, $F^{+}F^{-}$ pairs, charm baryon pairs, and associated charm production.

4C. The CERN Beam Dump Experiments

The beam dump experiments recently carried out at CERN are closely connected with the hadronic production of charmed particles because part or all of the observed signal can come from the neutrinos produced in charmed particle semi-leptonic decays. In these experiments, Fig. 24, a 400 GeV proton beam was dumped at zero degrees into a very thick target of copper followed by an iron absorber. About 400 m downstream there was the usual 400 m long muon shield used for the neutrino experiments. And further downstream was the three neutrino dectors (TABLE VII) BEBC, CDHS, and Gargamelle. The copper and iron dump suppresses the usual neutrino beam flux by a factor of 3000. Hence the three detectors are sensitive to these neutrinos (usually called prompt neutrinos) or other weakly interacting neutral particles which can be produced within an hadronic absoprtion length in the dump. The only presently known and sufficiently copious production mechanism is the creation and decay of charmed particles.

All three experiments observed events which had the characteristics of events produced in normal neutrino experiments. Hence the observed events are labeled ν_{μ}, ν_{e}, neutral current, and so forth. Most of the thinking about these events has indeed assumed that they are produced by ordinary neutrino; however we should keep in the back of our minds the thought that there is no direct proof that these are ordinary neutrinos or that they are neutrinos at all. The last line of TABLE VII gives the

$$p + \text{nucleon} \rightarrow D+\bar{D}+X \qquad (29)$$

production cross sections required to yield the anomalous portion of the observed events: the so-called prompt neutrino events. These calculations are model dependent and the individual references[50-55] must be consulted for the details.

The correctness of the hypothesis that the prompt neutrinos come from $D\bar{D}$ production can be examined by comparing the last line of TABLE VII with TABLE VI and with Eq. 28. I will make a few comments, but readers should make their own comparisons.

TABLE VII

CERN beam dump experiments. $\sigma_{D\bar{D}}$ which include $D^0\bar{D}$ and D^+D^- is calculated assuming that the nuclear $D\bar{D}$ production cross section is proportional to A. Note that some of the observed events are from conventional sources such as π's and K's which decay before interacting in the dump. The reference must be consulted to learn what fraction of the events are attributed to prompt neutrinos.

Detector		Gargamelle	BEBC	CDHS
Speaker at this conference.		F. Jacquet[50]	K. L. Wernhard[52]	P. Bloch[54]
Reference		51	53	55
Acceptance (10^{-6} sr		1.71	11.2	10.2
Mass of detector (metric tons)		10.5	13	450
Observed Events	ν_μ	12	29	727
	$\bar{\nu}_\mu$	2	5	160
	ν_μ or $\bar{\nu}_\mu$	2		
	ν_e		11	
	$\bar{\nu}_e$		4	
	ν_e or $\bar{\nu}_e$	9		
	Neutral current	7	21	
	Neutral current or ν_e or $\bar{\nu}_e$			261
$\sigma_{D\bar{D}}$ (μb/nucleon)		$80\ ^{+40}_{-25}$ (Ref.50)	120 ± 54 (Ref.56)	~ 30 (Ref.55) 40 ± 8 (Ref. 56)

(a) The $\sigma_{D\bar{D}}$'s required to explain the beam dump experiments prompt neutrino events, TABLE VII, are compatible with TABLE VI and Eq. 28 given the difficulties of the experiment and the uncertainties of the model used to calculate the cross sections. Furthermore the $\sigma_{D\bar{D}}$ in TABLE VII are overestimates because there will be some contributions to prompt neutrino events from F meson and charm baryon production.

(b) On the other hand, one should not get too comfortable with the comparison because the 95% confidence and 4 standard deviation upper limits in TABLE VI are the same size as the required cross

sections in TABLE VII. Clearly anomalous sources beyond charmed particle production are not excluded.

(c) There is a possible discrepancy between the bubble chamber measurements, BEBC and Gargamelle, and the CDHS measurement. This is most clearly seen in TABLE VIII taken from Jacquet's paper[50]. He defines

N_e = number of ν_e and $\bar{\nu}_e$ type events found.

$n_{e,prod}$ = number of ν_e and $\bar{\nu}_e$ neutrinos which had to be produced per proton in the beam dump to yield N_e

N_p = total number of protons

Ω = angular acceptance of detector with reference to beam dump (given in TABLE VII)

Since the ν_e and $\bar{\nu}_e$ total cross sections are proportional to E_ν, the neutrino energy, we can write

$$N_e = K \langle E_\nu \rangle n_{e,prod} N_p \quad , \tag{30}$$

where K is a constant for each detector. Then

$$\frac{n_{e,prod}}{\Omega} = \frac{N_e}{K\langle E_\nu \rangle N_p \Omega} \tag{31}$$

should be the same for all experiments.

TABLE VIII

Comparison of $n_{e,prod}/\Omega$. The errors are statistical and based only on N_e.

Detector	Gargamelle	BEBC	FHPRW
$K(GeV^{-1})$	2.45×10^{-12}	0.62×10^{-12}	20.1×10^{-12}
N_p	3.5×10^{17}	3.5×10^{17}	4.3×10^{17}
N_e	7.3	12	112*
$n_{e,prod}/\Omega$	$(4.6 \pm 1.7) \times 10^{-12}$	$(4.6 \pm 1.3) \times 10^{-2}$	$(1.2 \pm .11) \times 10^{-2}$

*Calculated from muonless events in Ref. 55

The combined results of the two bubble chambers differ from the CDHS result by 3 standard deviations.

4D. Neutrino Production of Charmed Particles

It is now well established[31),57)] that unlike sign dileptons events of the form

$$\nu_\mu + N \to \mu^- + \mu^+ + X \tag{32a}$$

$$\nu_\mu + N \to \mu^- + e^+ + X \tag{32b}$$

$$\nu_\mu + N \to \mu^- + \mu^+ + V^o + X \tag{32c}$$

$$\nu_\mu + N \to \mu^- + e^+ + V^o + X \tag{32d}$$

demonstrate the production of charmed particles in neutrino-hadron interactions. I shall not review this subject except to reproduce the nice compilation of Palmer[31)], Fig. 25, on the ratios

$$\frac{\text{Number } (\mu^- e^+ V^o)}{\text{Number } (\mu^- e^+)} \quad , \quad \frac{\text{Number } (\mu^- \mu^+ V^o)}{\text{Number } (\mu^- \mu^+)} \tag{33}$$

There has been some discussion[57)] as to whether the various measurements are consistent. Figure 25 makes two points.

(a) Given the large errors the various results are compatible.

(b) These ratios should increase as E_ν increases due to increased contributions from associated production of charmed particles and production of single charmed particles on quarks in the ocean.

Although events of the form of Eq. 32 are indirect evidence for charmed particle production; there is still a need for direct evidence based on reconstructing charmed particle invariant masses. Palmer[37)] reported that the decay mode $D^o \to K^o \pi^+\pi^-$ has been seen, Fig. 26, in the Columbus-BNL experiment using the 15 ft Fermilab bubble chamber in the wide band ν_μ beam. Their measured mass of $M_{Do} = 1850 \pm 15$ MeV/c^2 agrees with the SLAC-LBL measurement[42)] of $M_{Do} = 1863.3 \pm 0.9$ MeV/c^2.

4E. Conclusions for Section 4

The conclusions are obvious:

(a) A great deal more work must be done so that we have definitive measurements of the cross sections for the photoproduction, hadroproduction and neutrinoproduction of charmed particles.

(b) On the basis of the scanty existing measurements there is nothing obviously in conflict with our expectations as to the size or behavior of these cross sections.

(c) The events found in the CERN beam dump experiments may be completely explainable as due to prompt neutrinos from the decay of charmed particles, but that hypothesis is not yet proven.

5. SEARCHES FOR NEW PARTICLES

5A. Multilepton Events Produced by Neutrinos

In the past few years there has been a great deal of interest as to whether particles other than ordinary or charmed mesons are responsible for events of the form:

$$\nu_\mu + \text{Nucleon} \rightarrow \mu^- + \mu^+ + X, \text{ (unlike-sign dimuons)}; \tag{34a}$$

$$\nu_\mu + \text{Nucleon} \rightarrow \mu^- + \mu^- + X, \text{ (like-sign dimuons)}; \tag{34b}$$

$$\nu_\mu + \text{Nucleon} \rightarrow \mu^- + e^+ + X, \ (\bar{\mu}e^+ \text{ events}); \tag{34c}$$

$$\nu_\mu + \text{Nucleon} \rightarrow \mu^- + \mu^+ + \mu^- + X, \text{ (trimuons)}; \tag{34d}$$

and similar ν_μ induced events with more or other combinations of muons and electrons. By the time of this conference it had been generally agreed that the unlike sign dimuons and the $\mu^- e^+$ events could be completely explained by the production and decay of a charmed particle. This left the like-sign dimuons, Eq. 34b; the trimuons, Eq. 34d and events of the form

$$\nu_\mu + \text{Nucleon} \rightarrow \ell_1 + \ell_2 + \ell_3 + \ell_4 + X \tag{(34e}$$

(where ℓ_1, ℓ_2, ℓ_3, and ℓ_4 are muons or electrons) as the most intriguing places to search for new particles.

(a) Trimuon Events: These events were first reported in 1977 by Barish et al.,[58] and an important sample of 13 events has been described by the Fermilab-Harvard-Pennsylvania-Rutgers-Wisconsin (FHPRW) collaboration[59]. At this conference, K. Kleinknecht from the CERN-Dortmund-Heidelberg-Saclay (CDHS) collaboration reported[60] on 76 events. J. Smith[61] has presented a very thorough analysis of the trimuon events and my brief discussion here relies on his work.

Figure 27, the CDHS data[60], gives a beautiful overall picture of the relative rates of trimuon to single muon production. The rate $R(3\mu/1\mu)$ is given as a function on energy for their data in Fig. 28. Note that when corrected for the relative efficiency $R(3\mu/1\mu) \sim 10^{-4}$ for all E_{vis}. The

question is then whether this rate of trimuon events and their various kinematic distributions can be explained by conventional processes.

Two conventional processes are diagrammed in Fig. 29. In Fig. 29a a $\mu^+\mu^-$ pair is produced at the hadron vertex; the size and behavior of the pair production cross section being taken from experimental data on

$$\text{hadron} + N \to \mu^+ + \mu^- + X \tag{35}$$

These μ pairs tend to move in the direction of the produced hadrons; therefore in the transverse momentum plane they tend to move opposite in direction to the fast μ^-. The other conventional process, Fig. 29b is primarily μ pair production by internal bremsstrahlung from the first μ^-; hence these pairs move in the direction of the first μ^-. Smith[61] and Barger et al.[62] have discussed these diagrams in more detail.

Kleinknecht[60] and Smith[61] say that the number of trimuon events in the CDHS data can be explained by the processes in Fig. 29, and that these processes also explain the kinematic distributions of these events. For example: Fig. 30 shows that the very large 180° peak and smaller 0° peak in $\Delta\phi_{1,23}$ can be explained as the sum of these two processes. There is no need in the CDHS trimuon data to involve any new particles or unconventional processes.

Most of the published FHPRW trimuon events can be explained[62] by the two conventional processes in Fig. 29. However there are two so-called "super-events" with very large total muon energies and small total hadron energies in the FHPRW sample;[57),63] and these cannot be explained in this way. These events will remain a mystery unless more can be found.

(b) Like-sign Dilepton Events: T. Y. Ling[64] presented an extensive discussion of

$$\nu_\mu + N \to \mu^- + \mu^- + X \tag{36a}$$

events in the FHPRW data. The problem with these events is to show that they are not from

$$\nu_\mu + N \to \mu^- + \underbrace{\pi^- \text{ or } K^-}_{\hookrightarrow \mu^- + \bar{\nu}_\mu} + X \tag{36b}$$

FHPRW[64] finds that after correction of the background of Eq. 37

$$\frac{\text{Number}(\mu^-\mu^-)}{\text{Number}(\mu^-\mu^+)} = .10 \pm .07 \tag{37}$$

The simplest conventional explanation for $\mu^-\mu^-$ events is that they result from associated production of charmed particles (c and $\bar{c}$):

$$\nu_\mu + N \rightarrow \mu^- + \bar{c} + c + X \qquad (38)$$
$$\bar{c} \rightarrow \mu^-$$

where the c does <u>not</u> go to a detectable μ^+. CDHS has not yet published their data on $\mu^-\mu^-$ events and there is not yet enough other data on $\mu^-\mu^-$ events to decisively test this explanation[65].

(c) <u>Four-lepton Events</u>: Only a few four-lepton events are known. M. Holder et al.[66] have described a four-muon event; and H. J. Lubatti[67),68] at this conference described an event of the form

$$\bar{\nu}_\mu + N \rightarrow \mu^+ + e^- + e^+ + e^- + X \qquad (39)$$

The authors report[68] that they have no plausible interpretation of this event.

5B. <u>New Vector Mesons</u>

I have devoted this summary talk to relatively high energy phenomena and high mass particles. However in concluding this talk I want to emphasize that there are still new particles to be found in the lower mass range. In particular there is much work to be done in elucidating the number and properties of vector mesons in the 1 to 3 GeV/c^2 mass range. F. Laplanche[69] reviewed the research at the D.C.I. e^+e^- colliding beams facility; and M. Spinetti[70] described the work at ADONE. This area was recently reviewed at the Hamburg Conference[71] and therefore I will not review it here. However as an example of the kind of intricate structure that can exist I have reproduced (Fig. 31) preliminary results from the "$\gamma\gamma$" group[70] emphasizing the various structures near 1500 MeV. It was exciting to learn of the plans at Frascati to build a new high luminosity e^+e^- colliding beam facility ALA with a peak luminosity of 10^{31} cm^{-2}sec^{-1}, and capable of operating down to 1 GeV total energy.

5C. <u>Conclusions for Section 5</u>.

(a) Almost all trimuon events can be explained by conventional processes

(b) There may be a net $\mu^-\mu^-$ signal above background; however its size and properties require study and verification.

(c) We do not know if the trimuon "super-events" and the four-lepton events will lead us into the discovery of new particles.

6. ACKNOWLEDGEMENTS

I am very grateful to the many speakers at the conference who sent me advanced copies of their papers and figures so that I could write this talk.

7. REFERENCES

1. N. Cabibbo, these proceedings.
2. M. L. Perl, High Energy Hadron Physics (Wiley, New York, 1974), Chapter 20.
3. L. Hand in Proc. of 1977 Int. Symp. on Lepton and Photon Interactions at High Energy (DESY, Hamburg, 1977).
4. M. J. Alguard et. al., Phys. Rev. Lett. 37, 1261 (1976).
5. E. M. Riordan et al., SLAC-PUB 1634 (1975), W. E. Atwood, SLAC-185 (1975).
6. H. L. Anderson et al., Phys. Rev. Lett. 38, 1450 (1977).
7. C. Chang et al., Phys. Rev. Lett. 35, 901 (1975).
8. G. Alterelli, these proceedings.
9. T. Quirk, these proceedings.
10. W. Chen, these proceedings.
11. D. H. Perkins et al., Phys. Lett. 67B, 347 (1977).
12. For recent reviews see the papers by B. Barish and by P. Musset in Proc. of 1977 Int. Symp. on Lepton and Photon Interactions at High Energy (DESY, Hamburg, 1977).
13. A. Savoy-Navarro, these proceedings.
14. B. Tallini, these proceedings.
15. H. L. Anderson, H. S. Matis, and L. C. Myrianthopoulos, submitted to Phys. Rev. Lett. (1977); A. J. Buras et al., Nuc. Phys. B131, 308 (1977); A. J. Buras and K. J. F. Gaemers, CERN preprint TH 2322 (1977); O. Nachtmann in Proc. of 1977 Int. Symp. on Lepton and Photon Interactions at High Energy (DESY, Hamburg, 1977).
16. G. J. Feldman and M. L. Perl, Phys. Reports 19C, 234 (1975), Eq. 5.20.
17. G. Wolf, these proceedings.
18. G. Hanson, these proceedings and SLAC-PUB-2118 (1978).
19. G. J. Feldman and M. L. Perl, Phys. Reports 33C, 286 (1977), Sec. 2.
20. Y. Sacquin, these proceedings.
21. (a) I. Cohen et al., CLNS Preprint CLNS-378 (1977); (b) J. M. Scarr et al., DESY Preprint DESY-77/77 (1977).
22. For a more quantitative review see A. Seiden, T. L. Schalk and J. F. Martin, SLAC-PUB-2107 (1978), submitted to Phys. Rev. D.
23. R. Brandelik et al., Phys. Lett. 67B, 358 (1977).
24. For a review see Ref. 3 of this paper.
25. J. Bürger, these proceedings.
26. G. Grindhammer, these proceedings.
27. A. Diament-Berger, these proceedings.
28. R. Brandelik et al., Phys. Lett. 73B, 109 (1975).
29. J. Kirkby et al., to be published.
30. M. L. Perl in Proc. of 1977 Int. Symp. on Lepton and Photon Interactions at High Energy (DESY, Hamburg, 1977).
31. R. Palmer, these proceedings.
32. A. N. Cnops et al., Phys. Rev. Lett. 40, 144 (1978).
33. M. J. Murtagh in Proc. of 1977 Int. Symp. on Photon and Lepton Interactions at High Energy (DESY, Hamburg, 1977).
34. F. J. Heile et al., SLAC-PUB-2059 (1977), to be published in Nuc. Phys.
35. For a discussion of other assignments for ν_τ see S. P. Rosen, Phys. Rev. Lett. 40, 1057 (1978).

36. R. Devenish, paper presented at the Washington, D.C. meeting of the American Physical Society (April, 1978).
37. M. L. Perl et al., Phys. Lett. 70B, 487 (1977).
38. G. Feldman in Proc. of Int. Conf. on Neutrino Physics—Neutrinos 1978 (Purdue, 1978), to be published.
39. G. Alexander et al., Phys. Lett. 73B, 99 (1978).
40. J. Jaros et al., Phys. Rev. Lett. 40, 1120 (1978).
41. Y. S. Tsai, SLAC-PUB-2105; Phys. Rev. (to be published).
42. G. Feldman in Proc. of Summer Inst. on Particle Physics—1977 (SLAC Report 204).
43. J. M. Feller et al., Phys. Rev. Lett. 40, 274 (1978); J. M. Feller et al., LBL Preprint LBL-7523 (1978), submitted to Phys. Rev. Lett.
44. W. Bacino et al., Phys. Rev. Lett. 40, 671 (1978).
45. R. Brandelik et al., Phys. Lett. 70B, 132 (1977).
46. D. Lüke, SLAC-PUB-2086 (1978), to be published in Proc. of 1977 Meeting of Division of Particles and Fields of American Physical Society (Argonne, 1977).
47. M. Piccolo et al., Phys. Rev. Lett. 39, 1503 (1977).
48. F. Richard, these proceedings.
49. B. Barish et al., CIT preprint CALT 68-655 (1978).
50. F. Jacquet; these proceedings.
51. P. Aliban et al., Phys. Lett. 74B, 134 (1978).
52. K. L. Wernhard, these proceedings.
53. P. C. Bosetti et al., Phys. Lett. 74B, 143 (1978).
54. P. Bloch, these proceedings.
55. T. Hansl et al., Phys. Lett. 74B, 139 (1978).
56. K. Schultze, talk given at Stanford Linear Accelerator Center, May 1978.
57. D. Cline in Proc. of 1977 Int. Symp. on Lepton and Photon Interactions at High Energy (DESY, Hamburg, 1977).
58. B. C. Barish et al., Phys. Rev. Lett. 38, 577 (1977).
59. A. Benvenuti et al., Phys. Rev. Lett. 38, 1110 (1977), 40, 432, 488 (1978).
60. K. Kleinknecht, these proceedings.
61. J. Smith, these proceedings.
62. V. Barger et al., Preprint COO-881-32 (1978).
63. D. D. Reeder in Proc. of 1977 Int. Symp. on Lepton and Photon Interactions at High Energy (DESY, Hamburg, 1977).
64. T. Y. Ling, these proceedings.
65. If the explanation is correct, then associated charm production will be a major contribution to the trimuon event ratio, contrary to the discussion in Sec. 5A.a.
66. M. Holder et al., Phys. Lett. 73B, 105 (1978).
67. M. J. Labatti, these proceedings.
68. R. J. Loveless et al., Preprint COO-088-29 (1978).
69. F. Laplanche, these proceedings.
70. M. Spinetti, these proceedings.
71. See papers by F. Laplanche and by C. Bemporad in Proc. of 1977 Int. Symp. on Lepton and Photon Physics at High Energy (DESY, Hamburg, 1977).

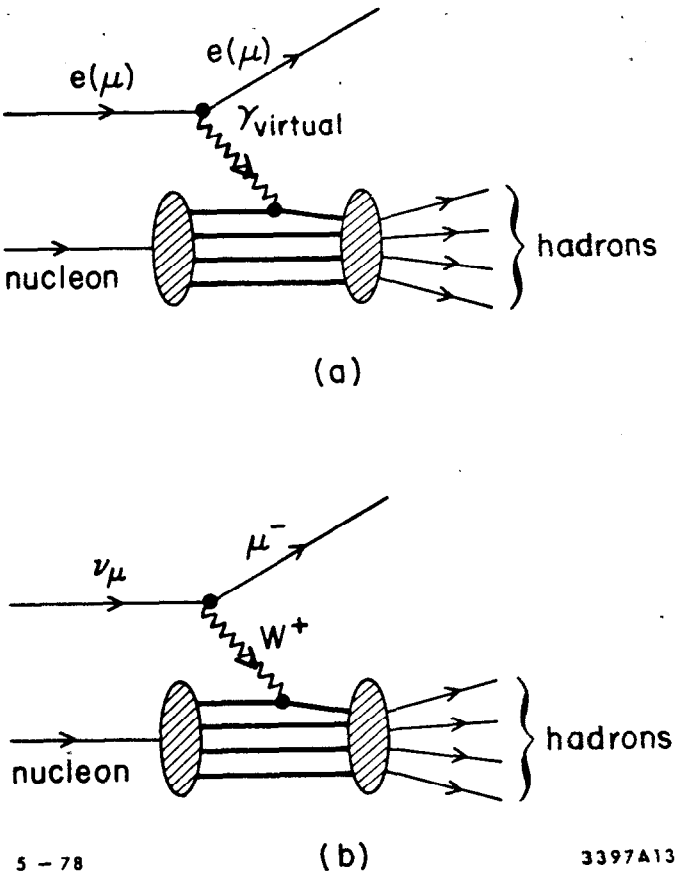

Fig. 1. The quark-parton model for (a) deep inelastic electroproduction or muoproduction; and (b) deep inelastic neutrinoproduction.

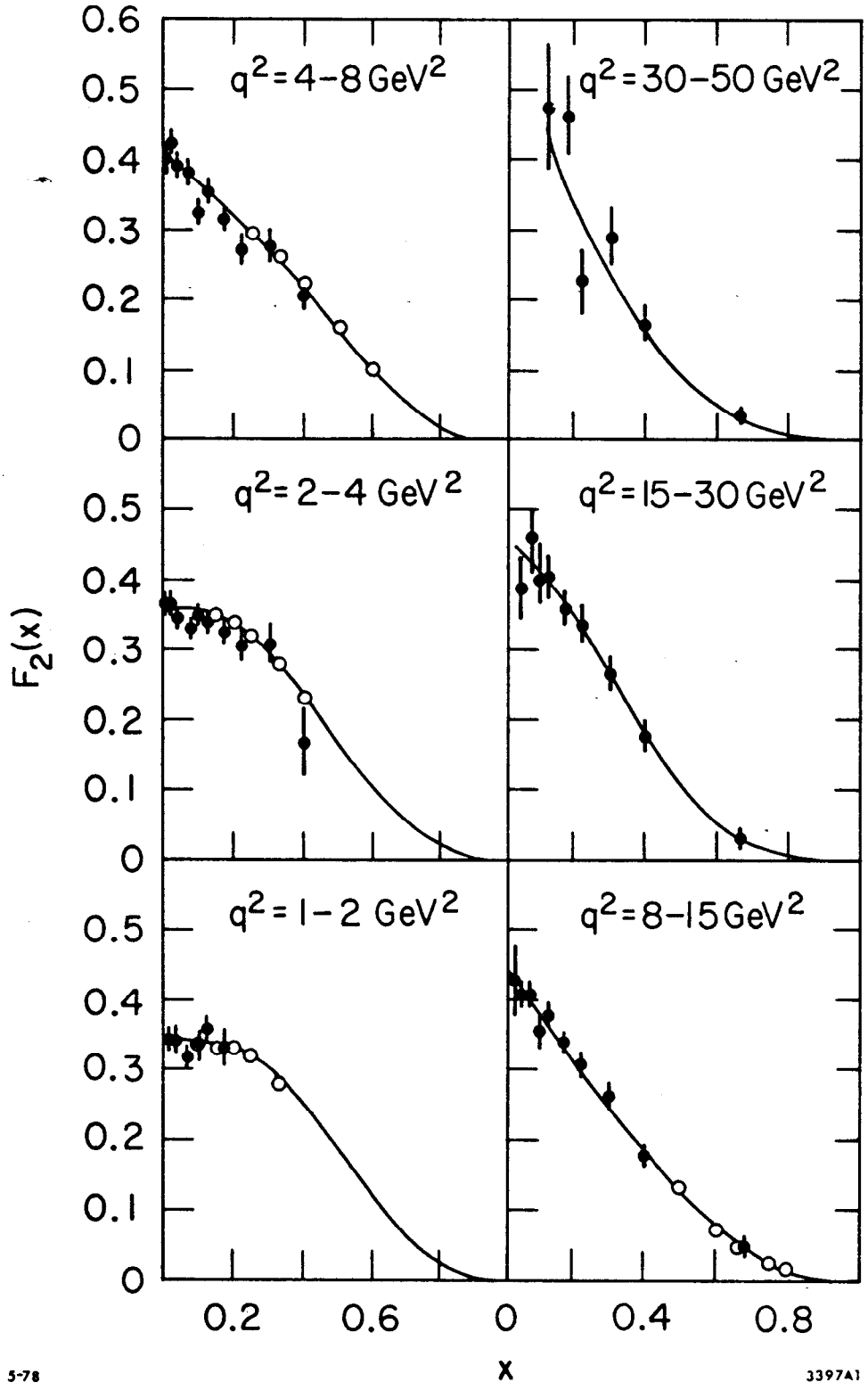

Fig. 2. F_2^{em} versus x. The solid circles are from μ-p deep inelastic scattering at 147 GeV (Ref. 9). The curves are fits (Ref. 9) to the lower energy electron data shown by the open circles (Ref.5).

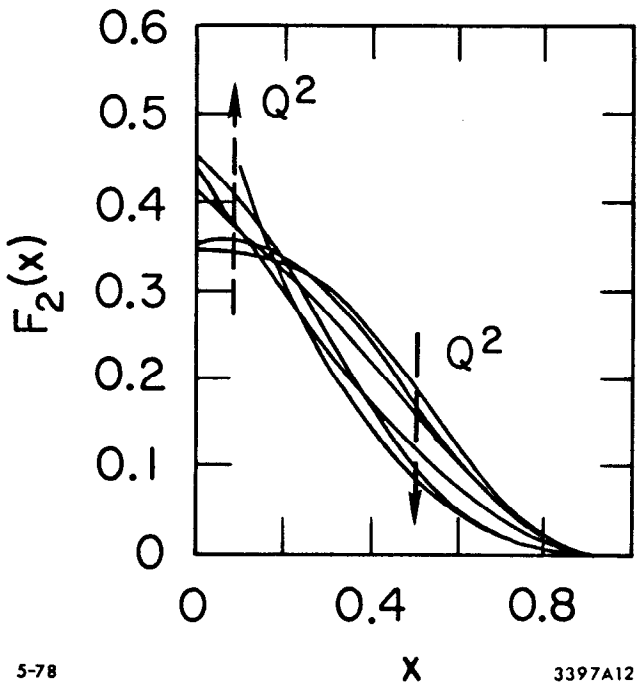

Fig. 3. A superposition of the curves from Fig. 2.

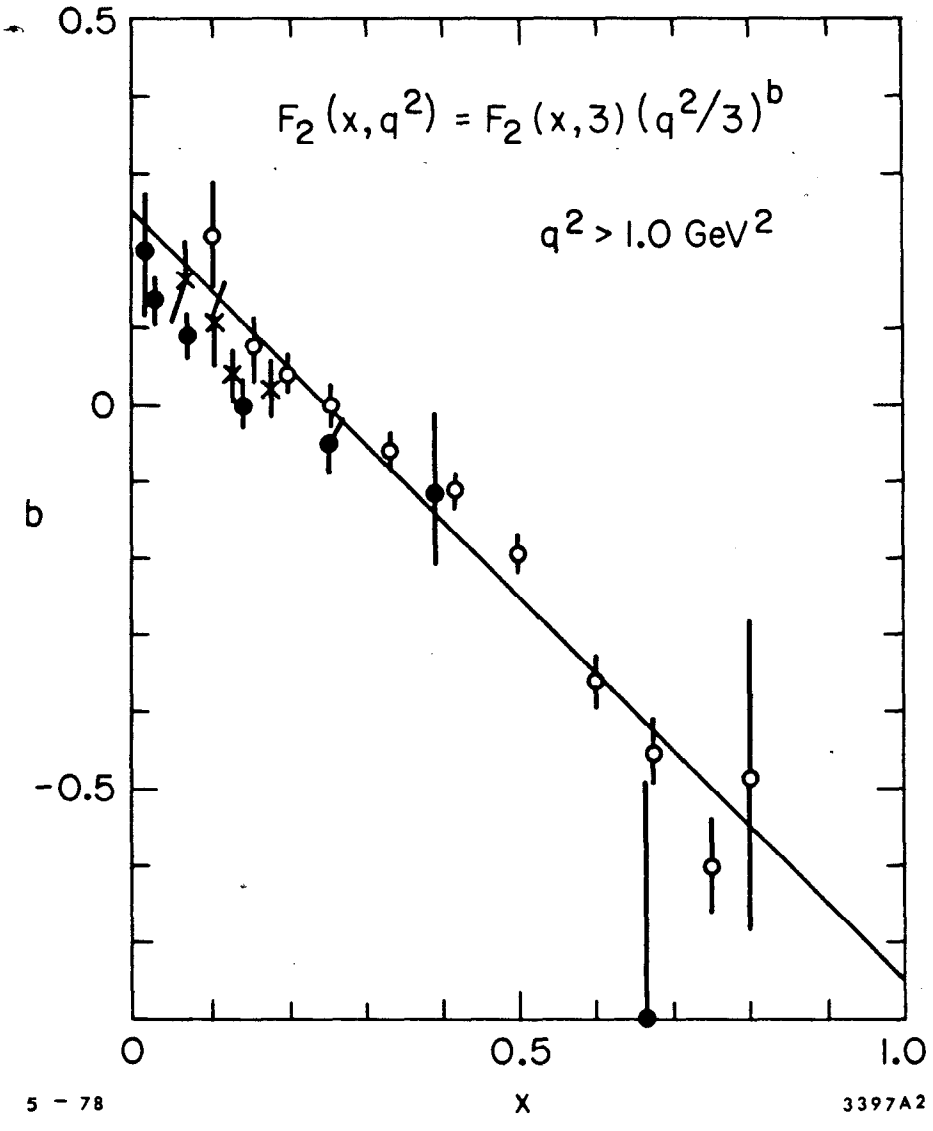

Fig. 4. Comparison of Eq. 6 using $q_0^2=3$ and b=0.25-x for: lower energy e-p data (open circles, Ref. 5); 147 GeV μ-p data (solid circles, Ref.9); 147 GeV μ-Fe data (x's, Ref. 6). Prepared by T. Quirk.

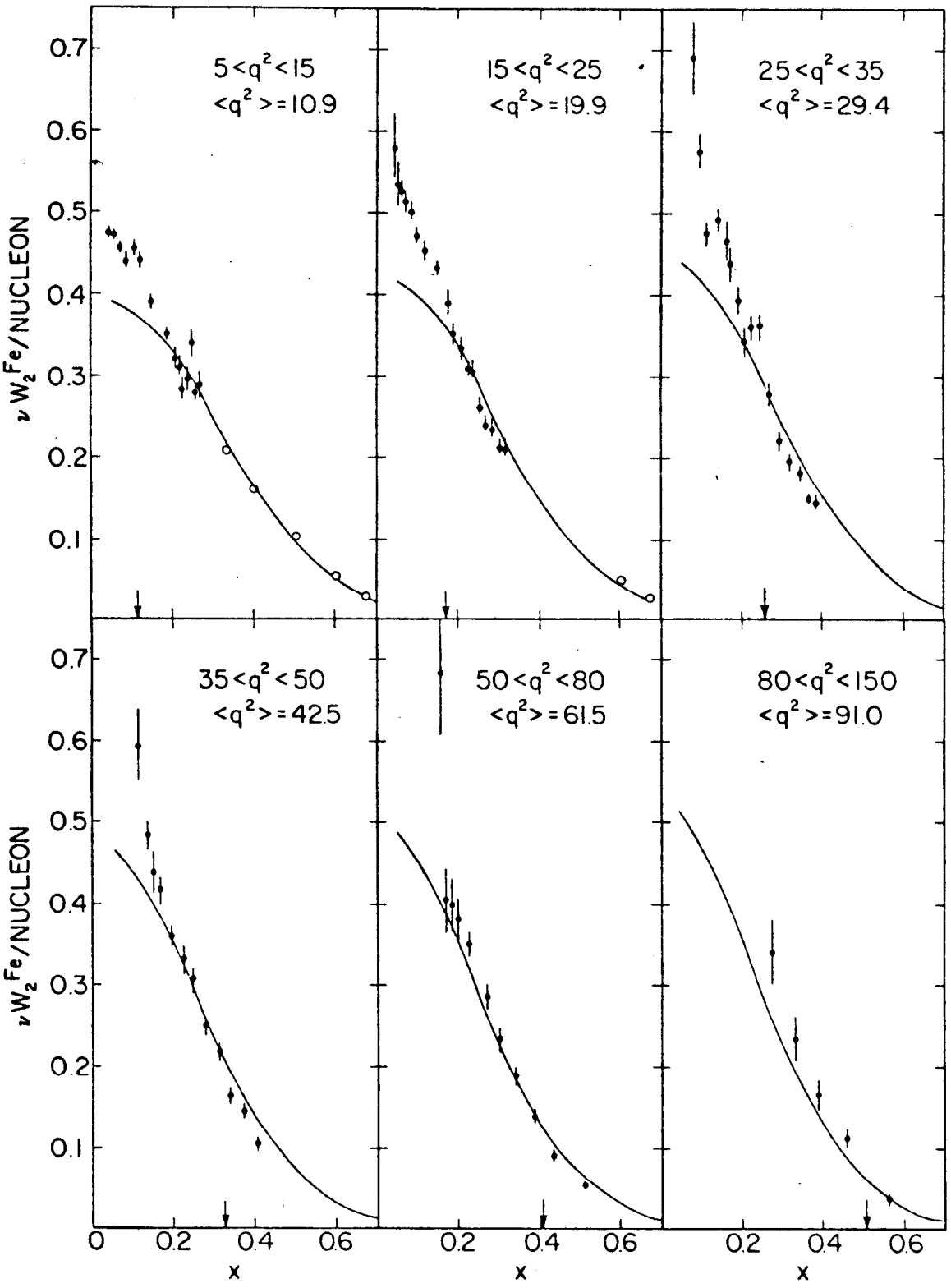

Fig. 5. $\nu W_2 = F_2^{em}$ versus x from μ-Fe data at 270 GeV. νW_2 is given per nucleon. The μ-Fe data and the curves which fit lower energy e-p data are from W. Chen, Ref. 10.

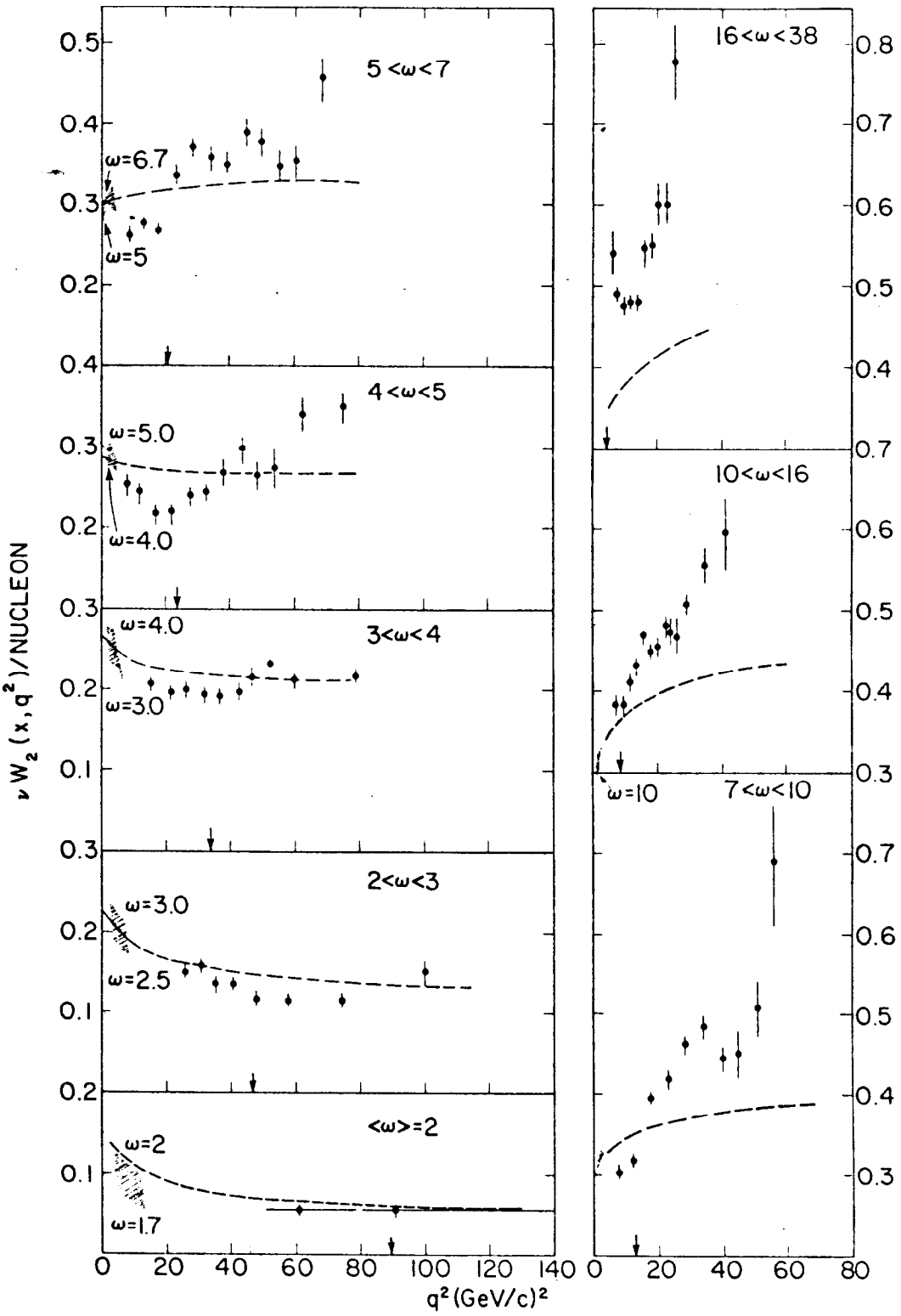

Fig. 6. $\nu W_2 = F_2^{em}$ versus q^2 for μ-Fe data at 270 GeV, from W. Chen, Ref. 10.

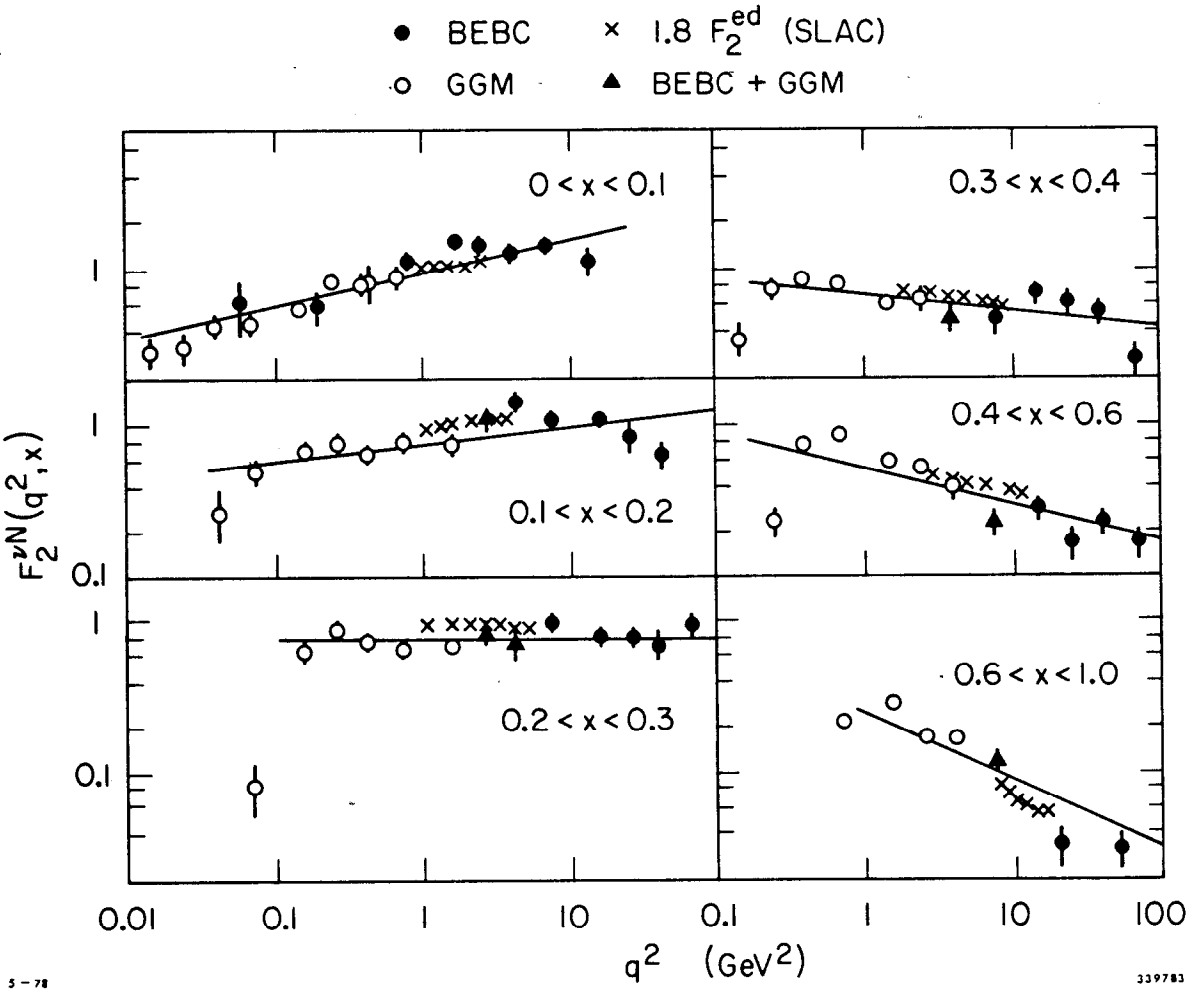

Fig. 7. Comparison of F_2 for neutrinoproduction and electroproduction versus q^2 presented by B. Tallini, Ref. 14. F_2^{em} is multiplied by 1.8 in accordance with the quark model.

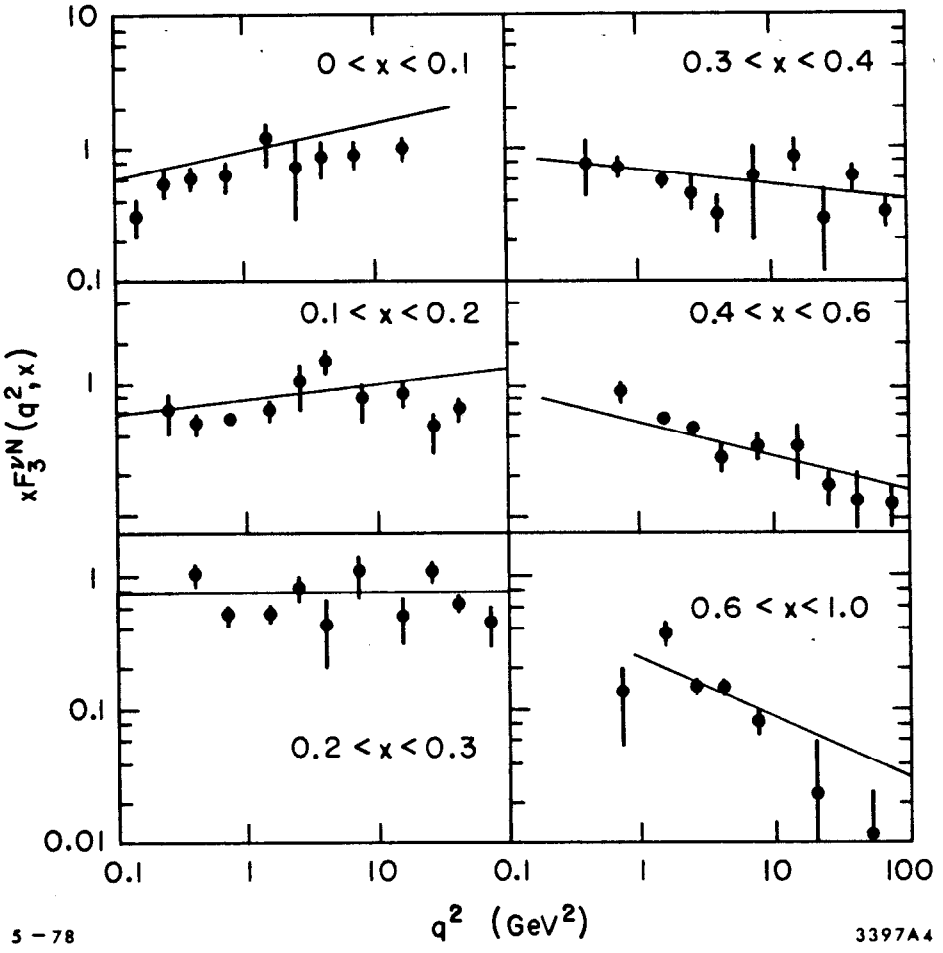

Fig. 8. $xF_3^{\nu N}$ versus q^2 from Ref. 14.

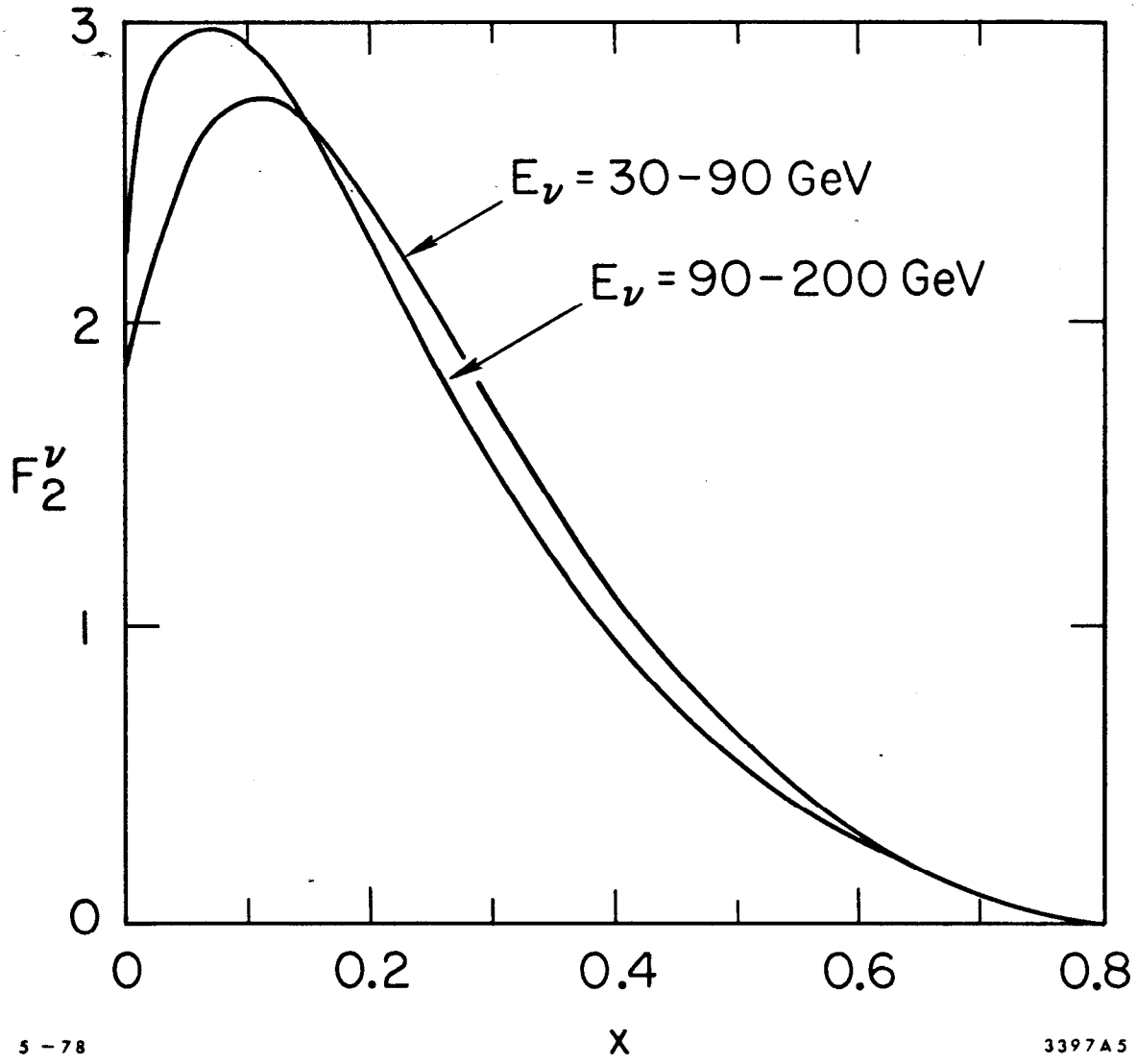

Fig. 9. F_2^{ν} versus x for two different E_ν regions from Ref. 13.

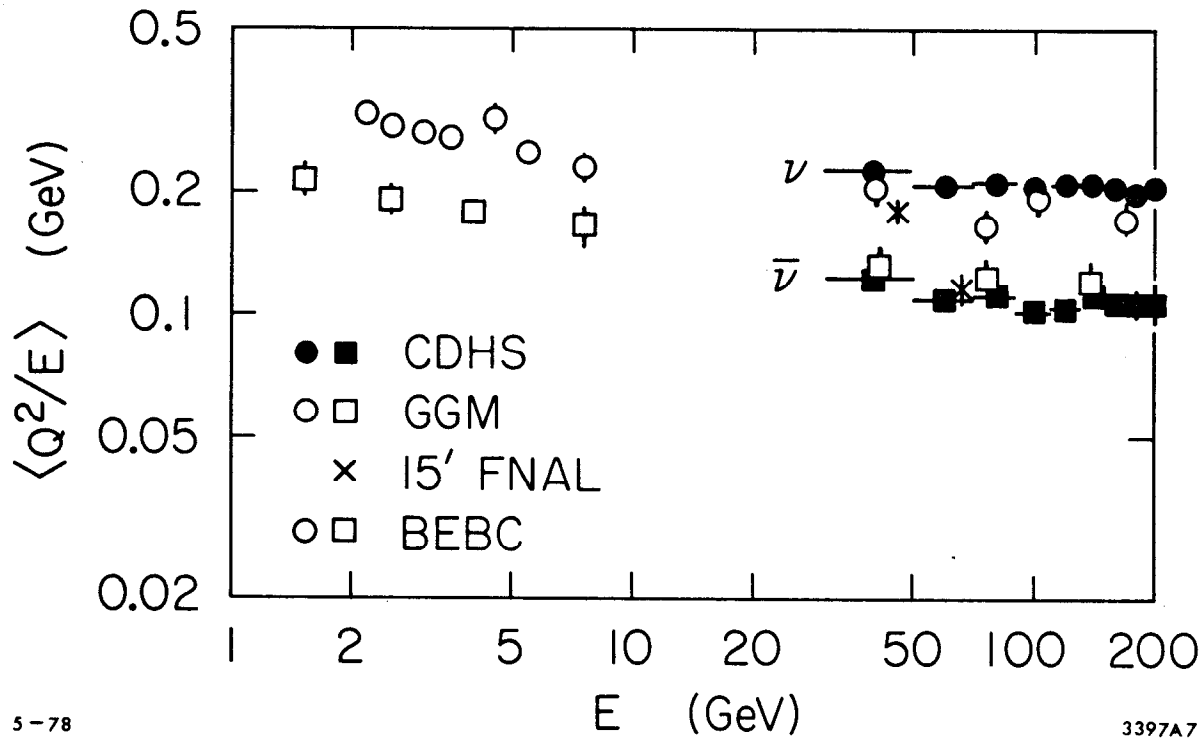

Fig. 10. $\langle Q^2/E_{\nu,\bar{\nu}} \rangle$ versus the neutrino energy E presented by A. Savoy-Navarro, Ref. 13.

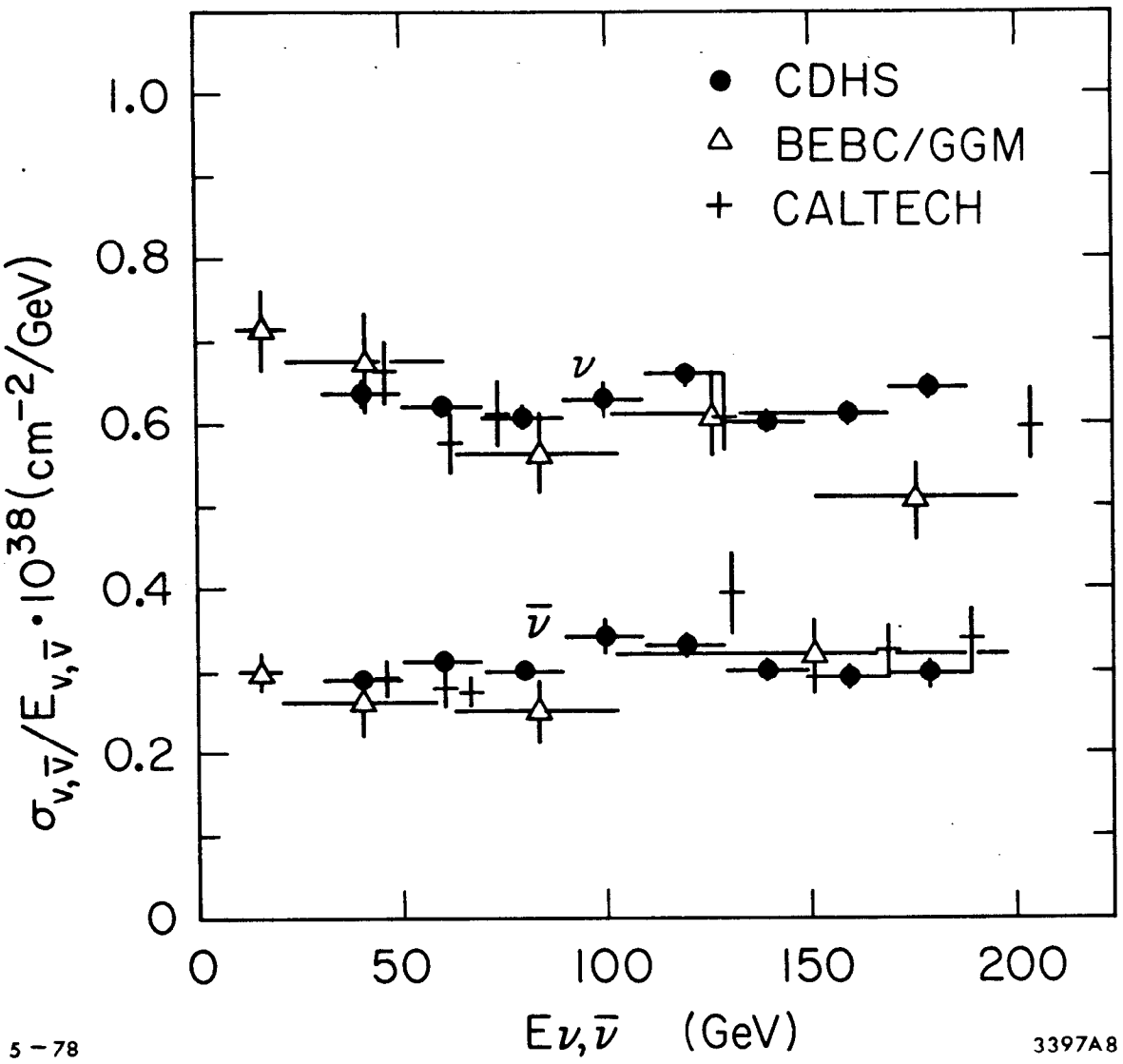

Fig. 11. $\sigma_{\nu,\bar{\nu}}/E_{\nu,\bar{\nu}}$ versus the neutrino energy E from Ref. 13.

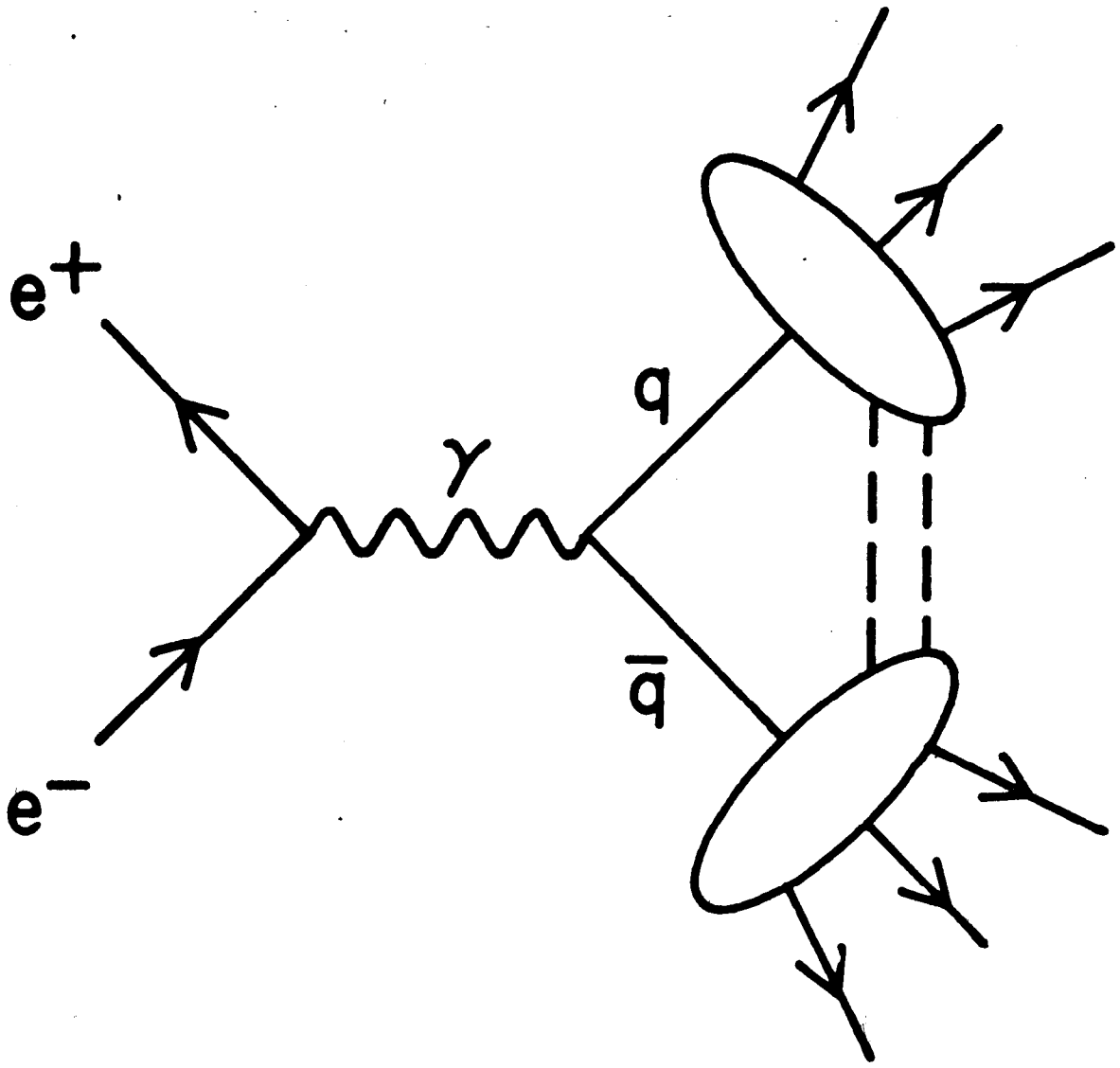

Fig. 12. Timelike virtual photon production of hadrons.

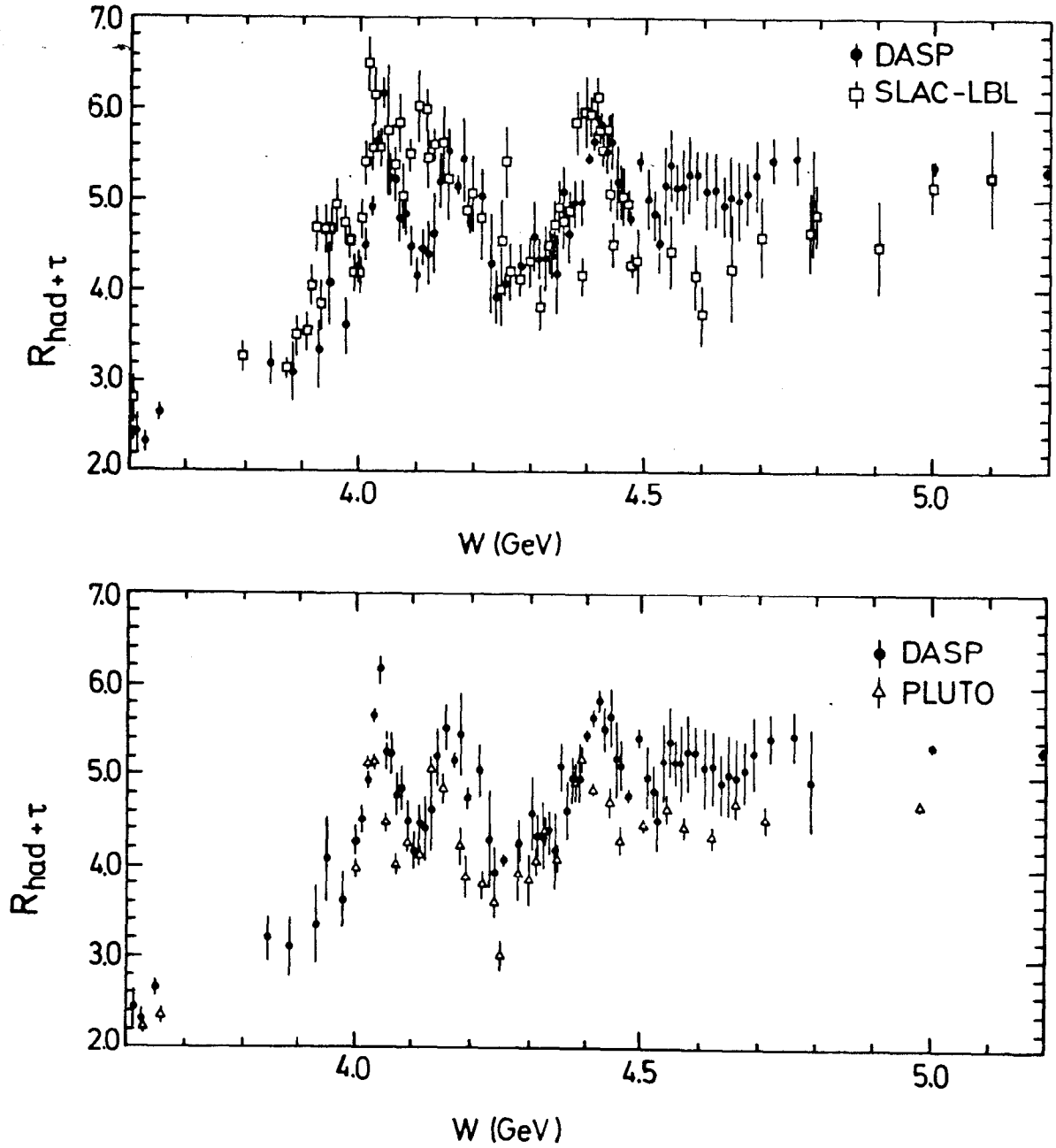

Fig. 13. The total $R=R_{had} + R_{\tau}$ versus the total center-of-mass energy W from DASP; presented by G. Wolf (Ref. 17).

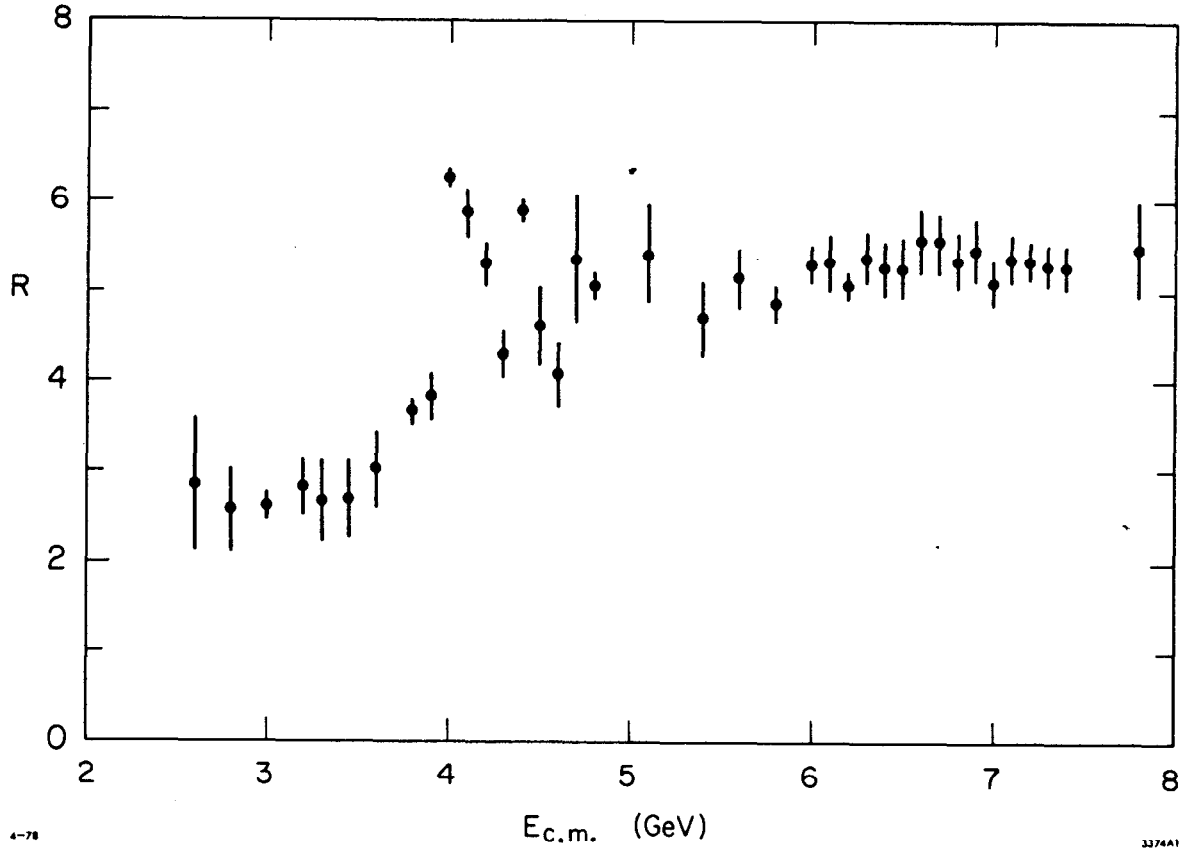

Fig. 14. The total R versus the total center-of-mass energy $E_{c.m.}$ from the SLAC-LBL Collaboration; presented by G. Hanson (Ref. 18).

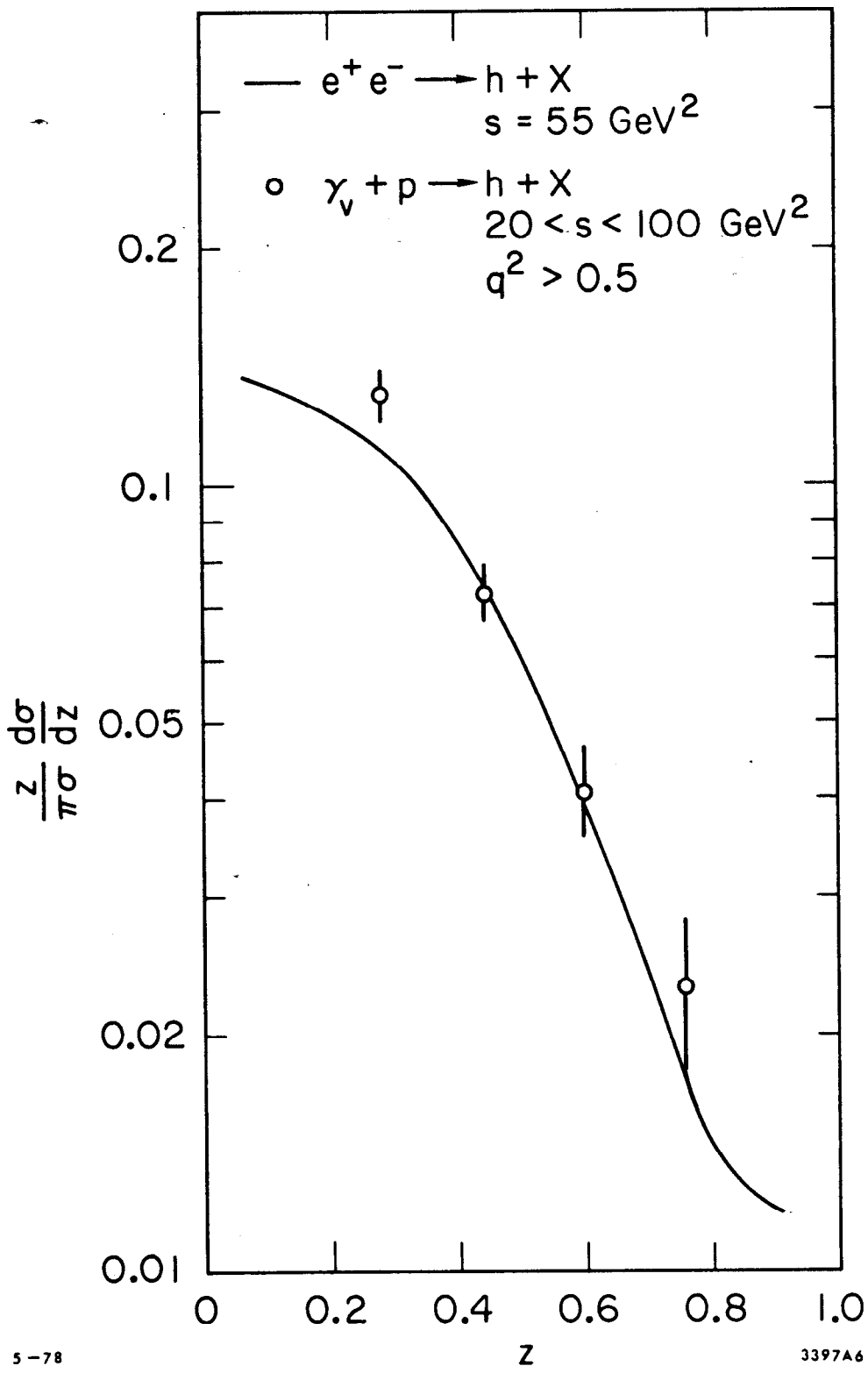

Fig. 15. Comparison of $(z/\pi\sigma)(d\sigma/dZ)$ versus z for the single hadron inclusive distributions from e^+e^- annihilation and muoproduction. Prepared by T. Quirk, Ref. 9.

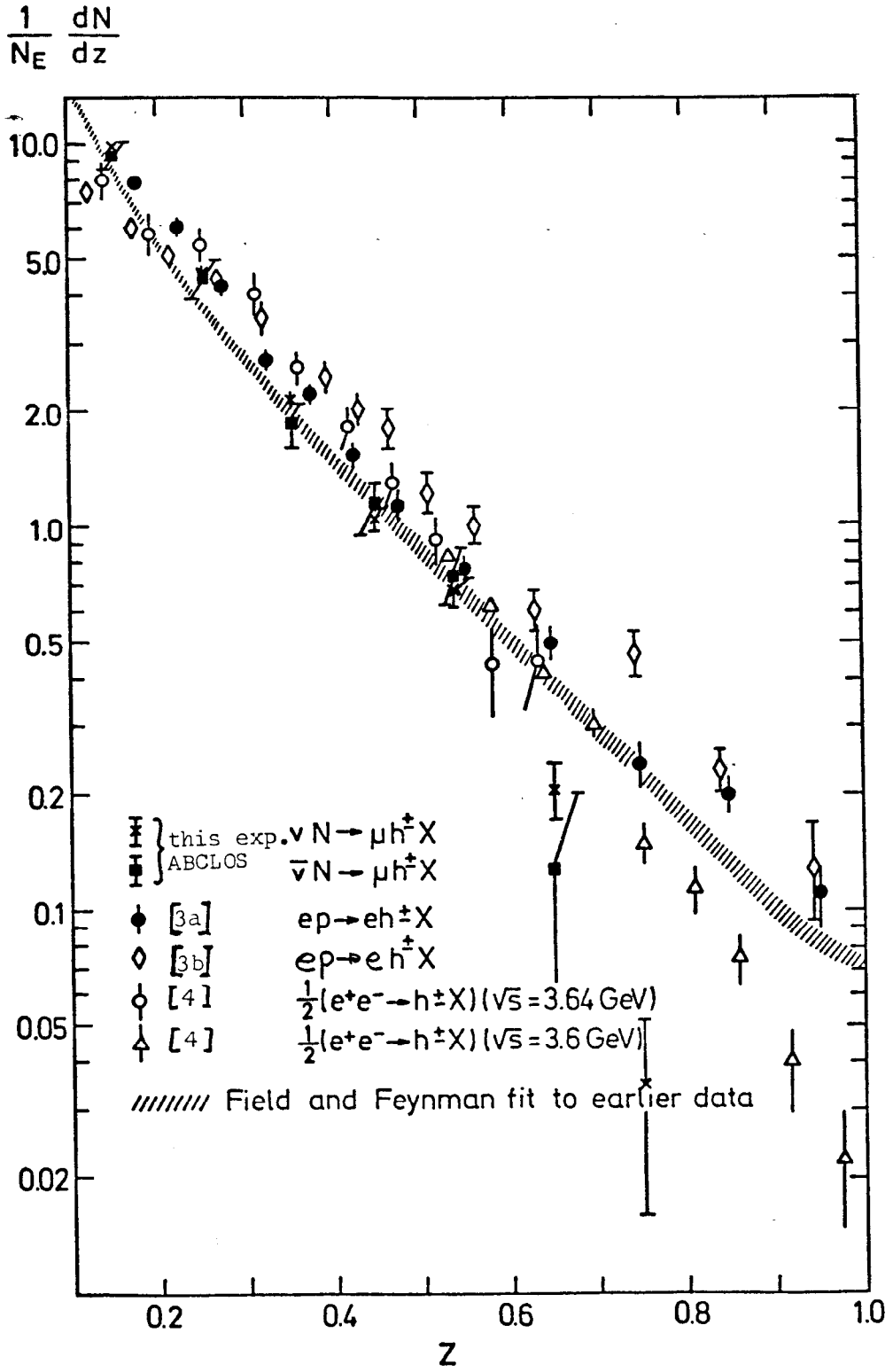

Fig. 16. Comparison of (1/N)(dN/d) versus z for neutrinoproduction, electroproduction, and e^+e^- annihilation from Y. Sacquin Ref. 20.

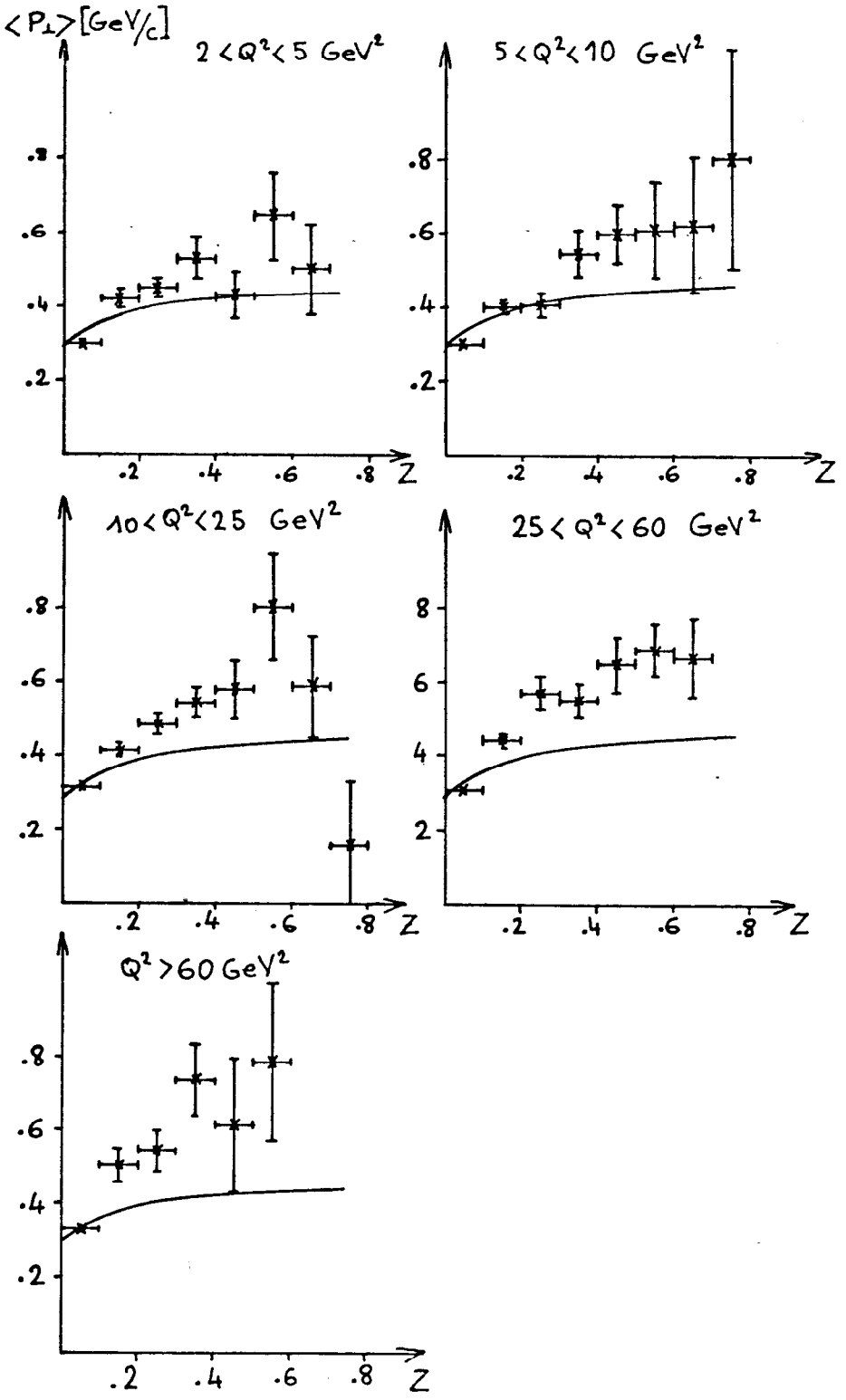

Fig. 17. $\langle P_\perp \rangle$ versus z for neutrinoproduction in various Q^2 ranges, Ref. 20.

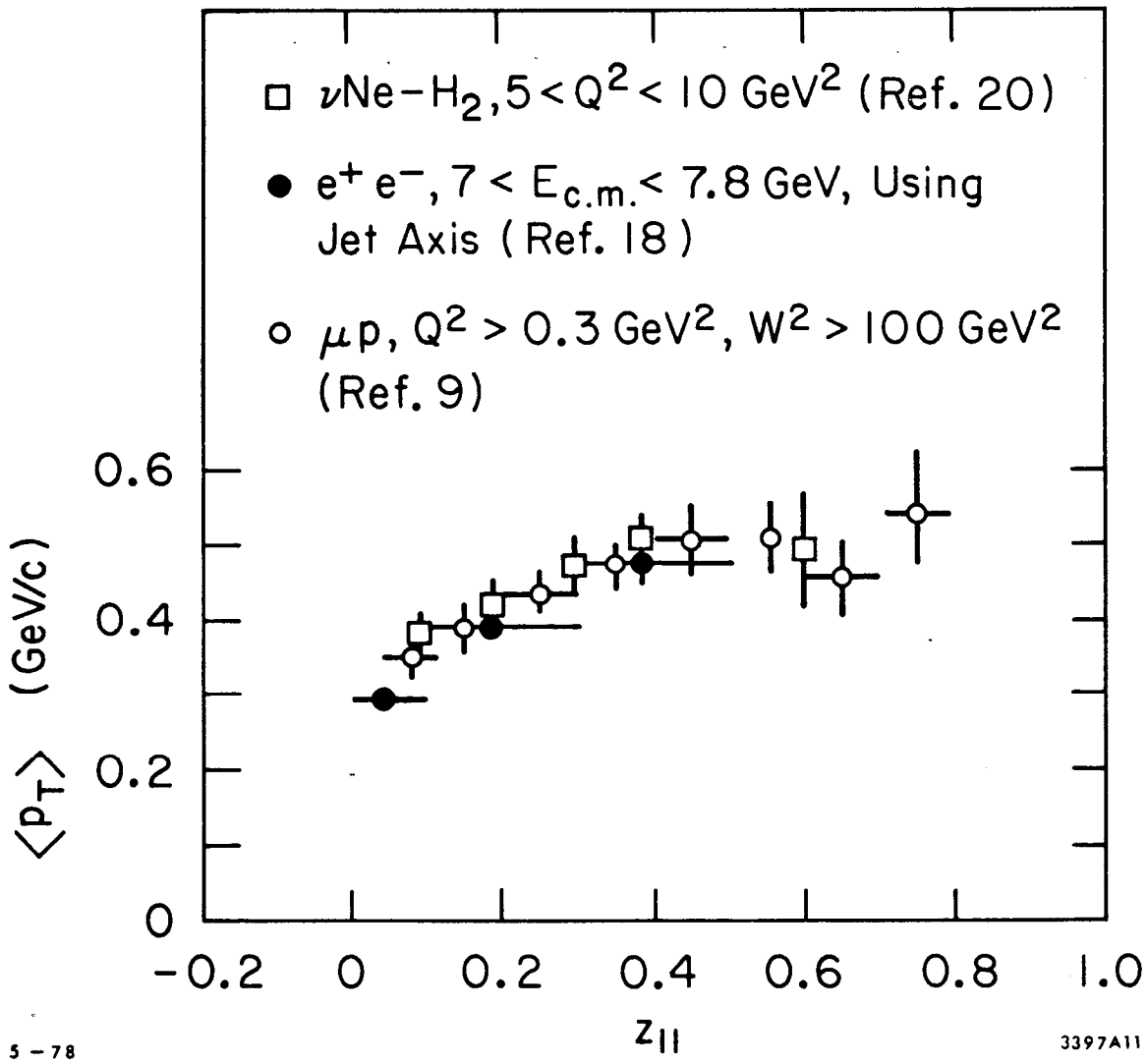

Fig. 18. Comparison of $\langle P_T \rangle$ versus z for neutrinoproduction, muoproduction and e^+e^- annihilation.

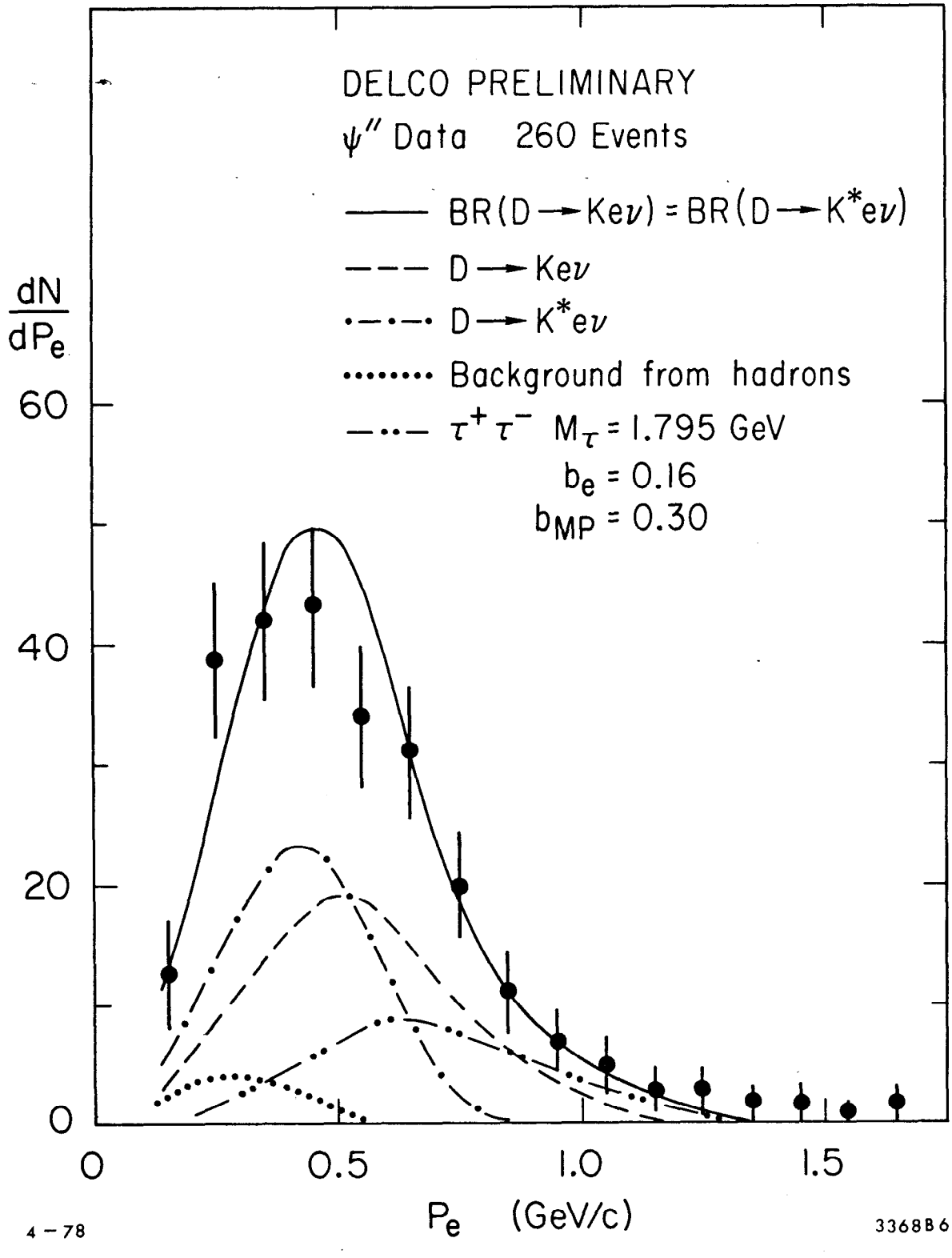

Fig. 19. The $e^{\pm}$ momentum spectrum for D decay from DELCO, Ref. 27.

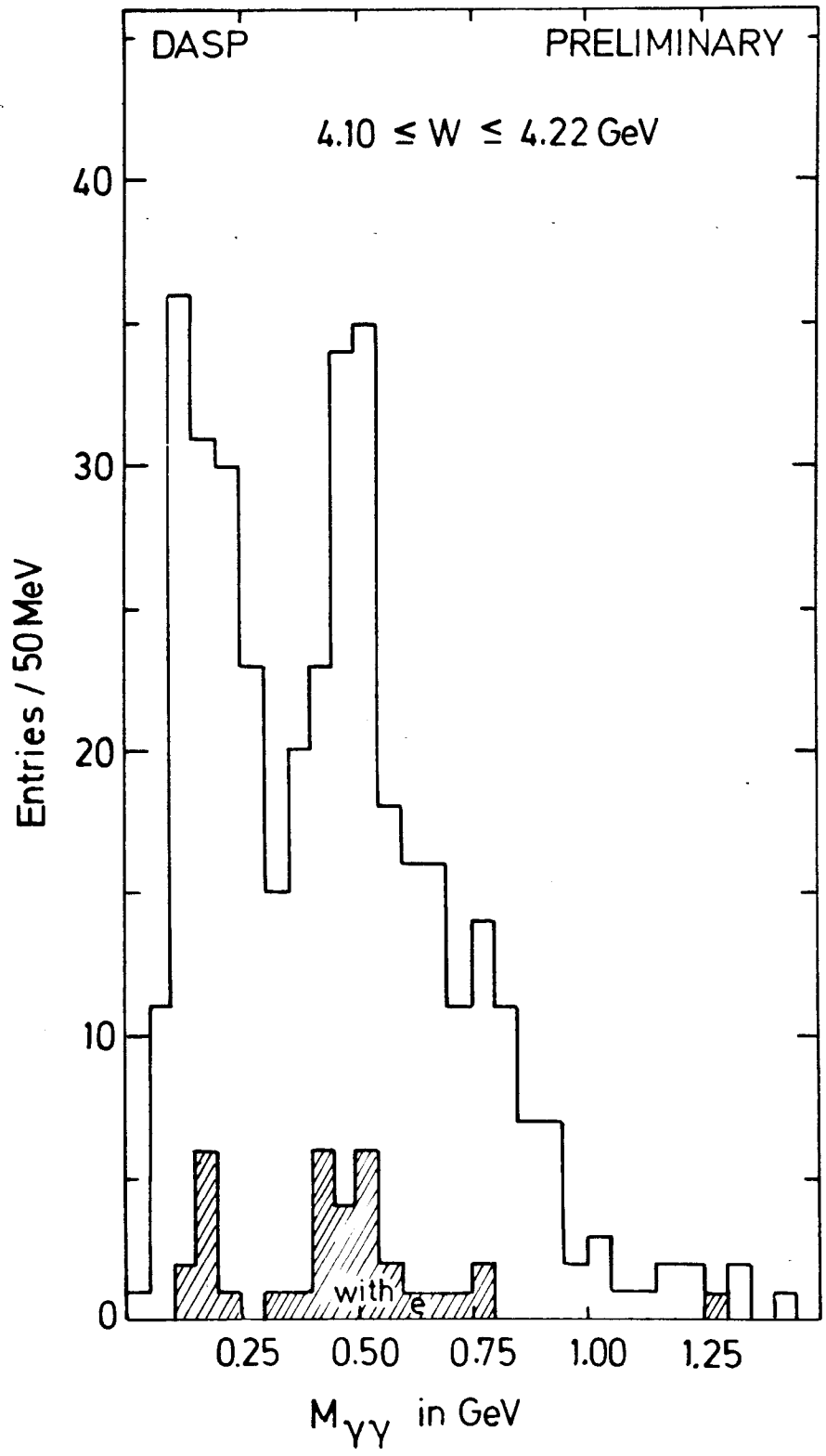

Fig. 20. The 2γ invariant mass spectrum in the energy range of 4.10 to 4.22 GeV showing a π^0 and an η peak; from DASP, Ref. 17.

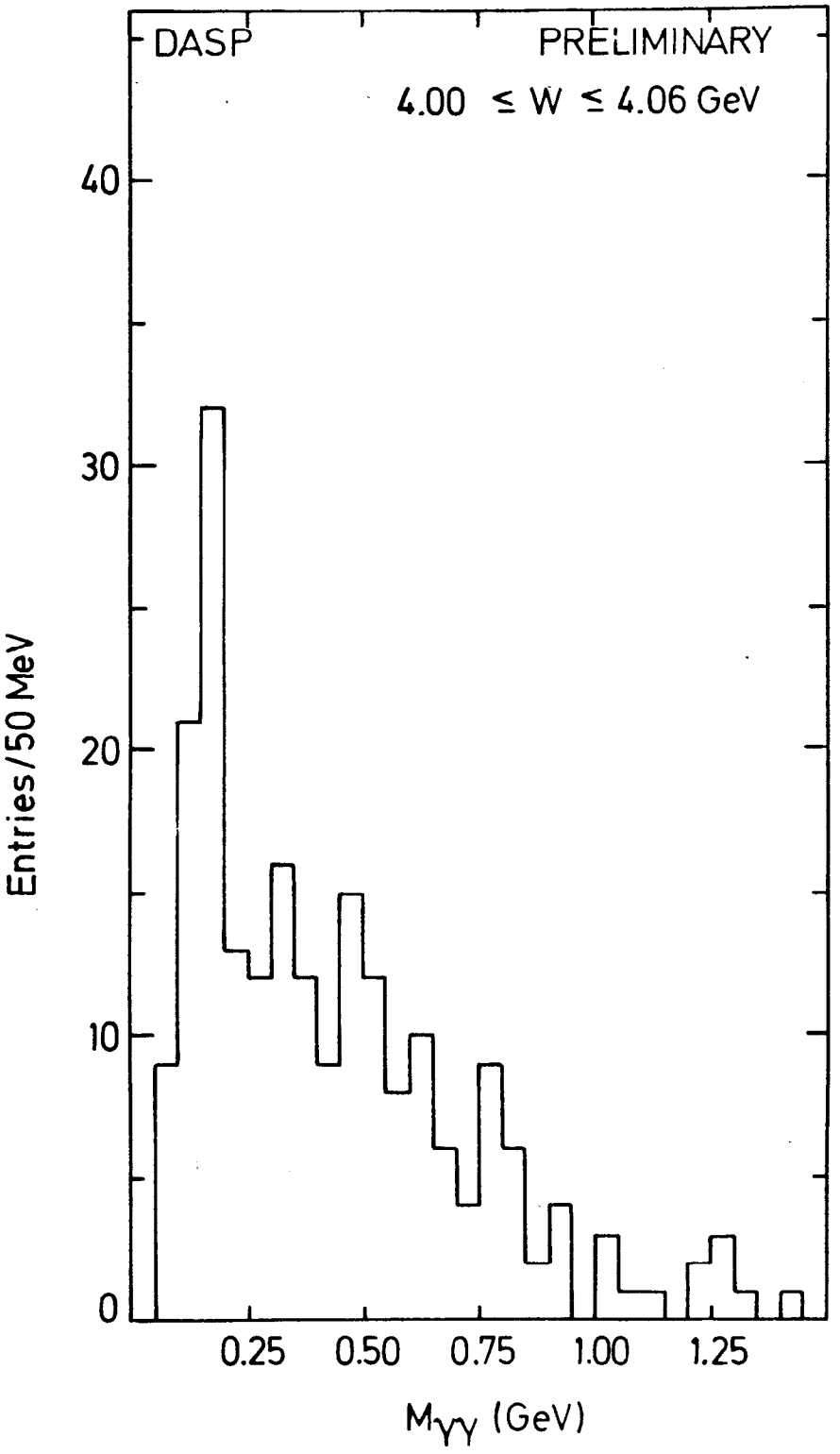

Fig. 21. The 2γ invariant mass spectrum in the energy range of 4.00 to 4.06 GeV showing only a π^o peak; from DASP, Ref. 17.

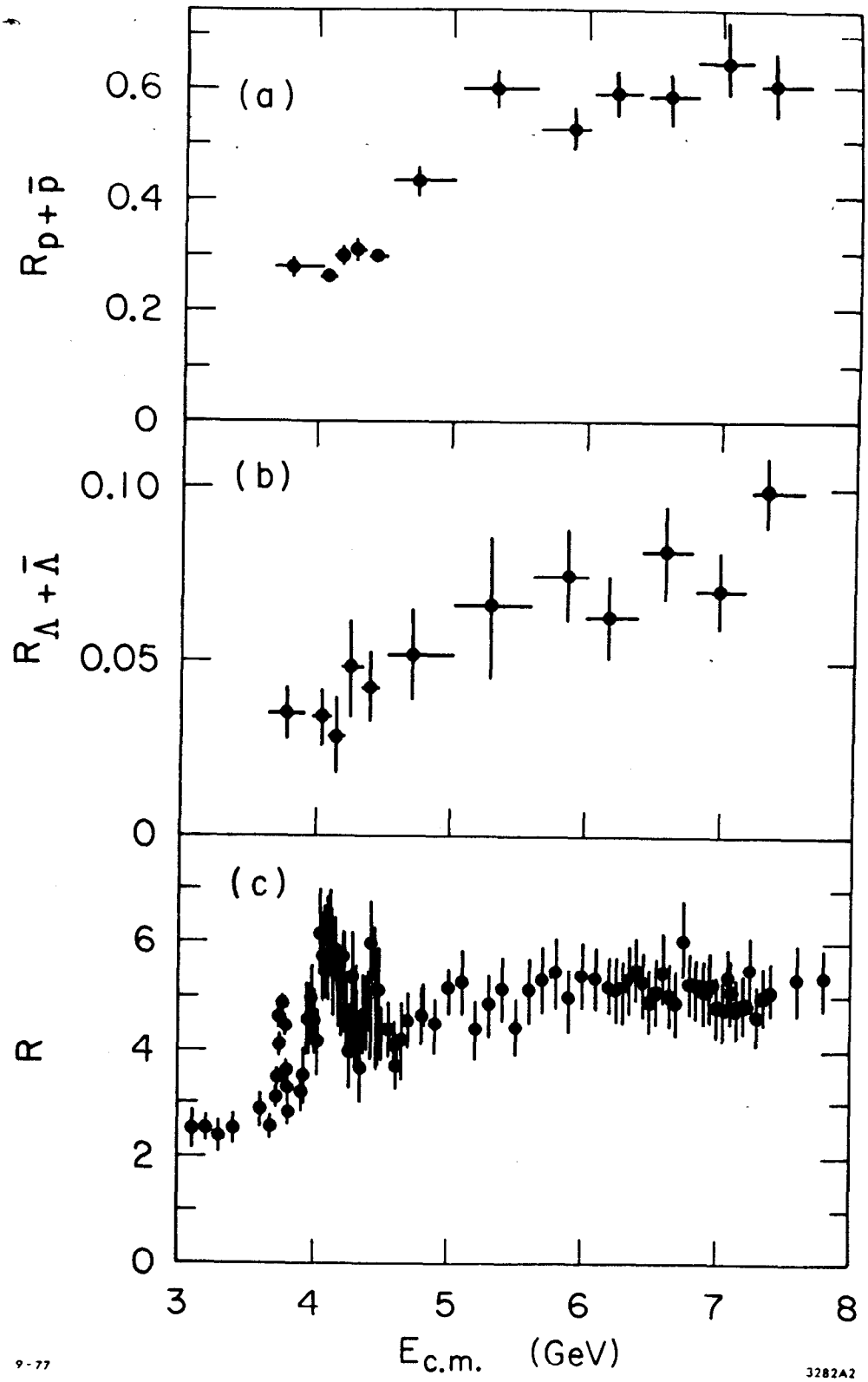

Fig. 22. R for (a) inclusive $p + \bar{p}$ production, (b) inclusive $\Lambda+\bar{\Lambda}$ production, and (c) total particle production versus $E_{c.m.}$ (Ref. 47).

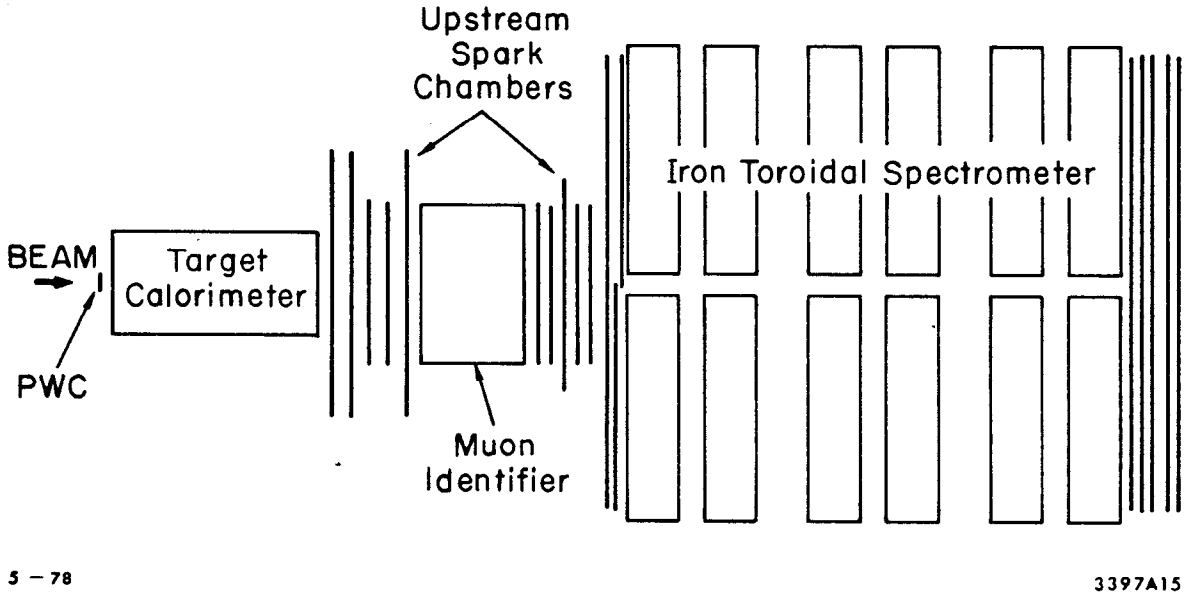

Fig. 23. The apparatus (not to scale) used for the CIT-Stanford measurement of charmed particle production by observation of a single prompt muon (Ref. 49).

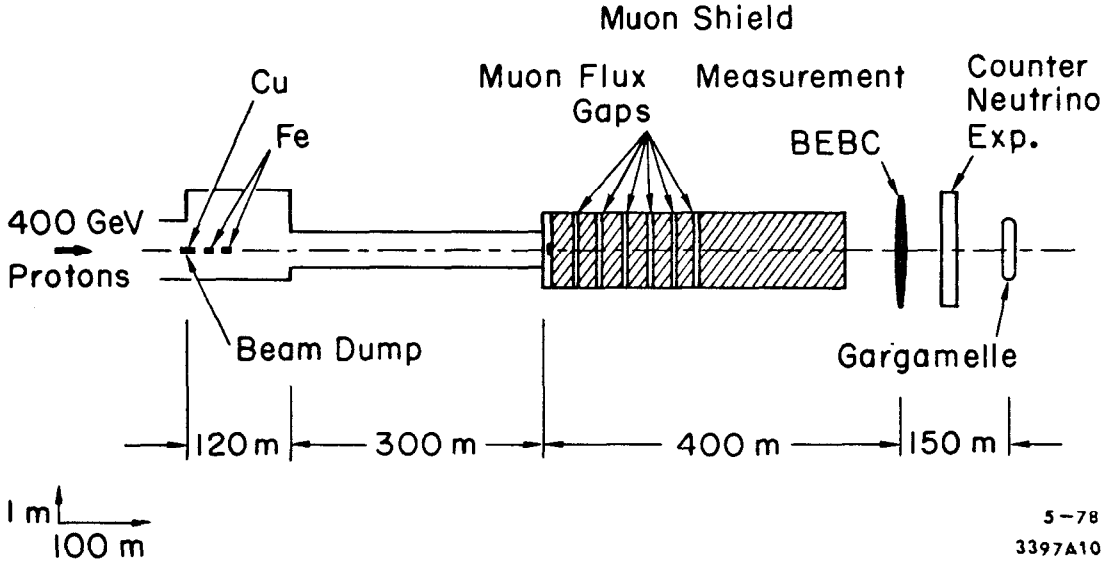

Fig. 24. The layout of the CERN beam dump experiments.

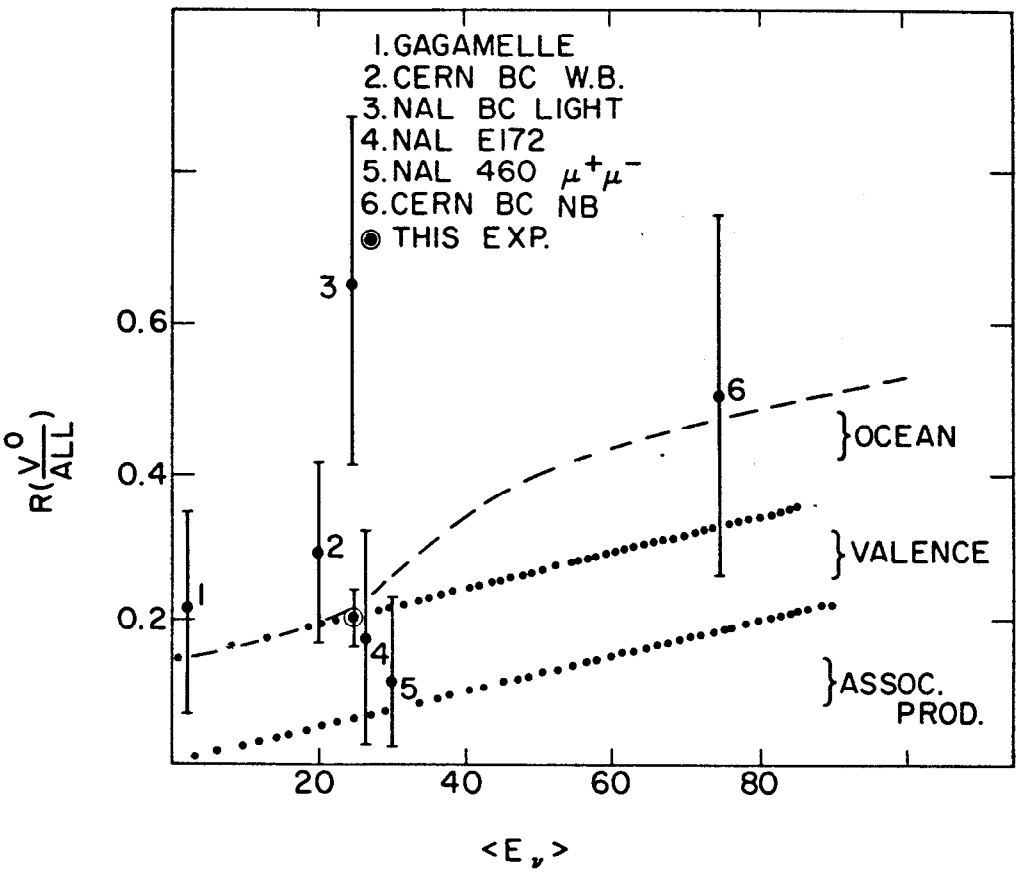

Fig. 25. Comparison of the number of unlike-sign dilepton neutrino events with and without V^0's versus the neutrino energy for various experiments. Compiled by R. Palmer, Ref. 31.

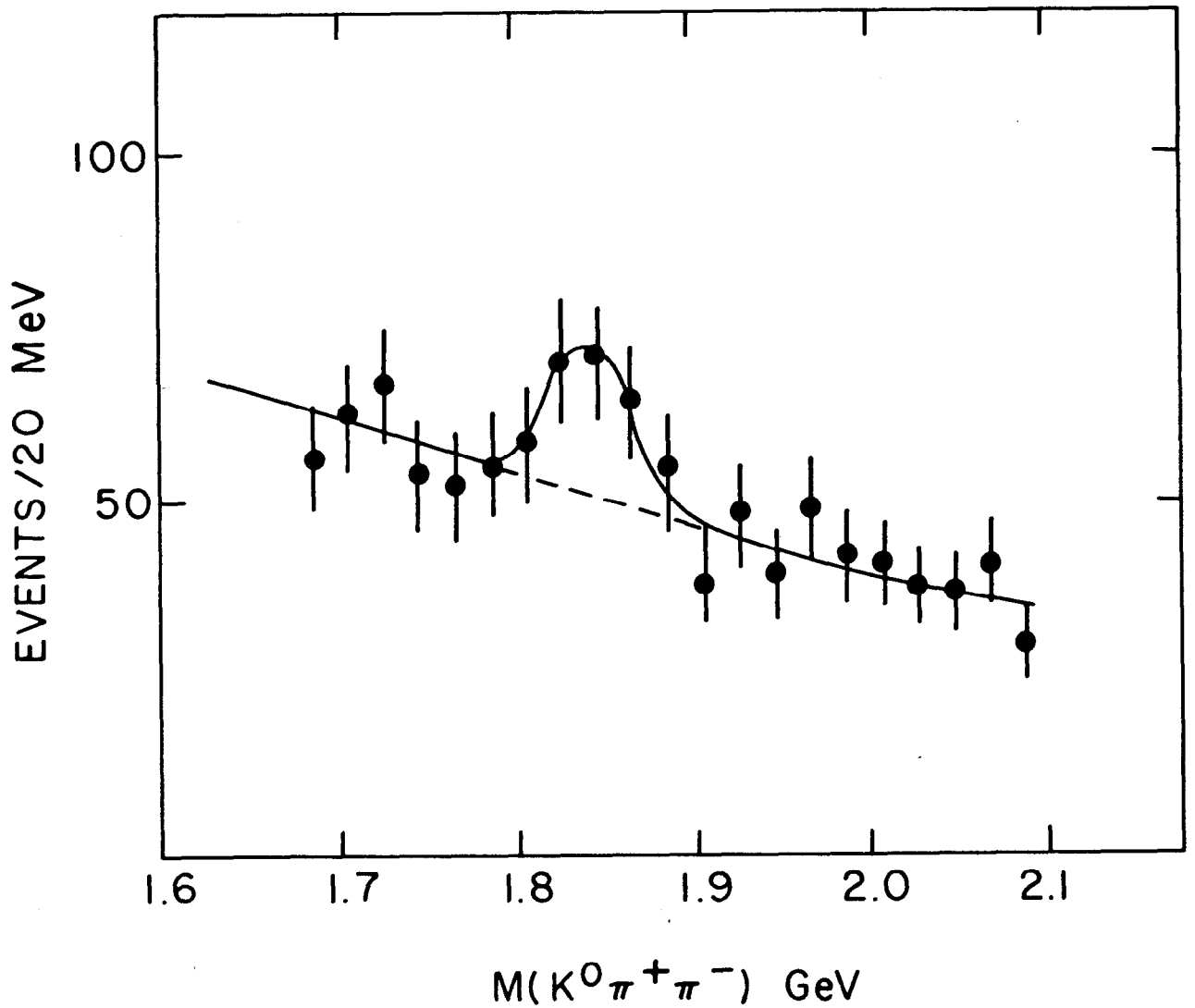

Fig. 26. Evidence for neutrino production of a D^0 which decays into the $K^0\pi^+\pi^-$ state (Ref. 31).

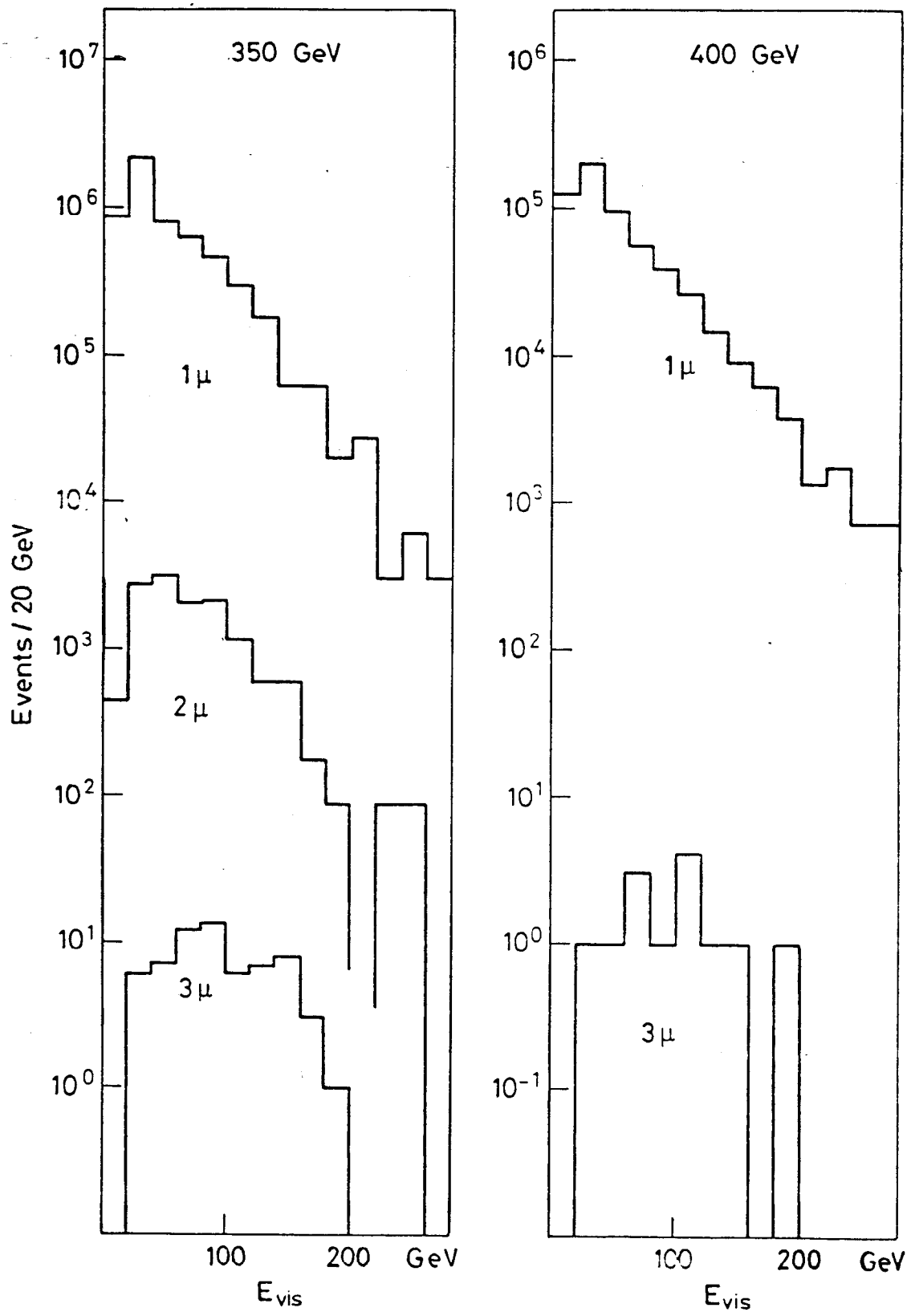

Fig. 27. Relative production of 1μ, 2μ, and 3μ events versus E_{vis} from the CDHS experiment (Ref. 60). These production rates are not corrected for detection efficiency.

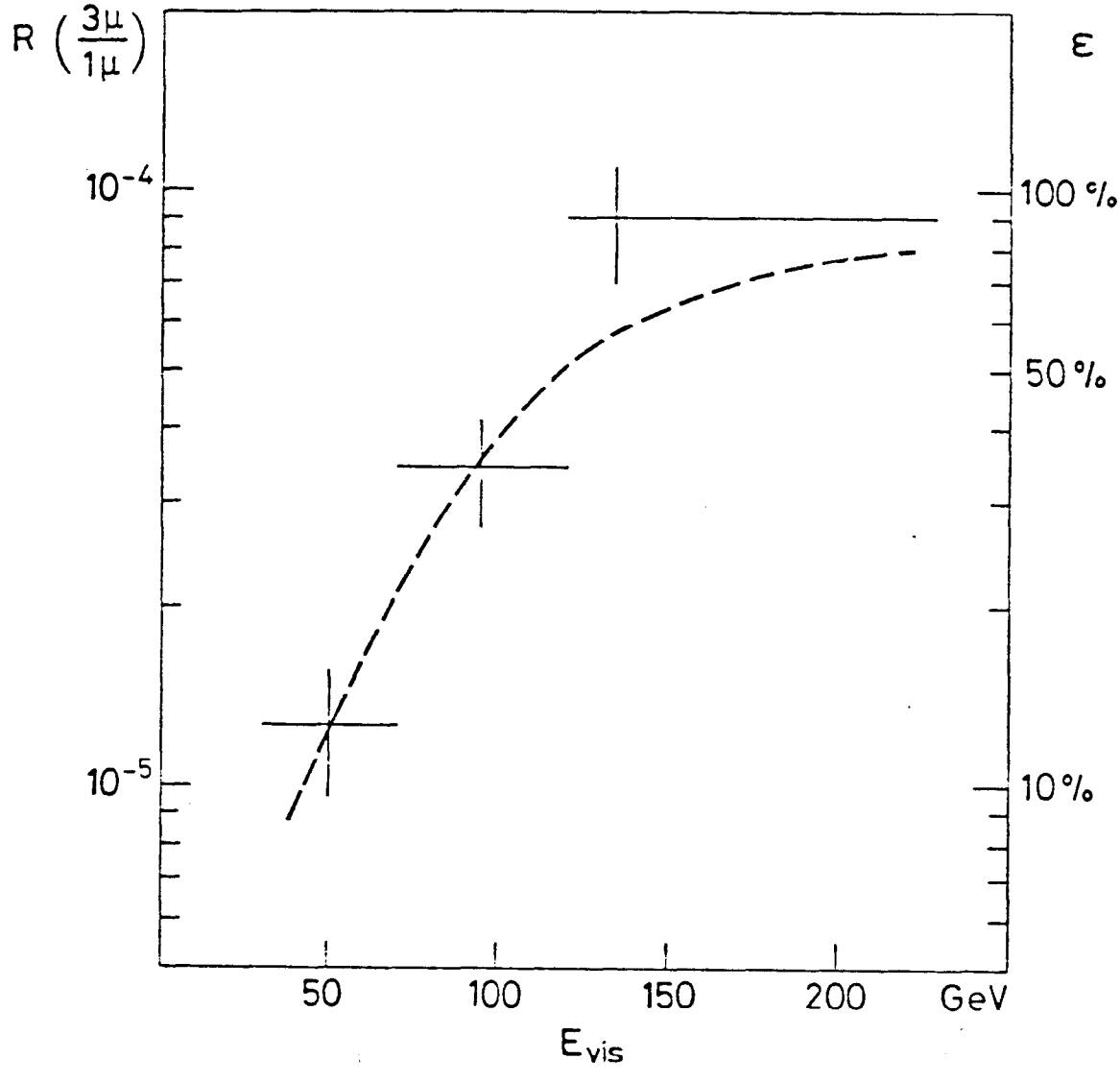

Fig. 28. Comparison of the ratio of 3μ to 1μ event production with the 3μ detection efficiency for the CDHS experiment (Ref. 60).

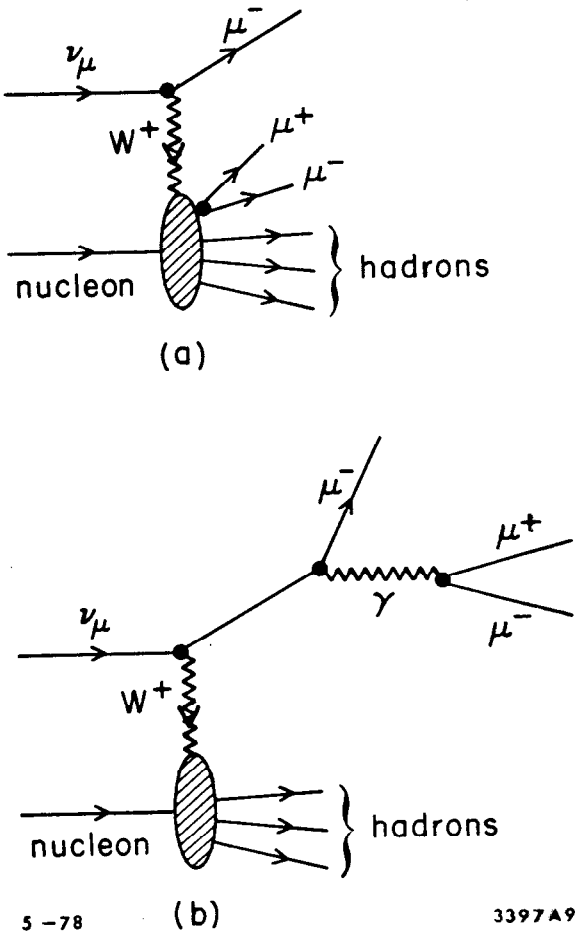

Fig. 29. Diagrams for production of trimuon events by (a) $\mu^+\mu^-$ pair production at the hadron vertex; and by (b) $\mu^+\mu^-$ pair production thru bremsstrahlung of the primary μ^-.

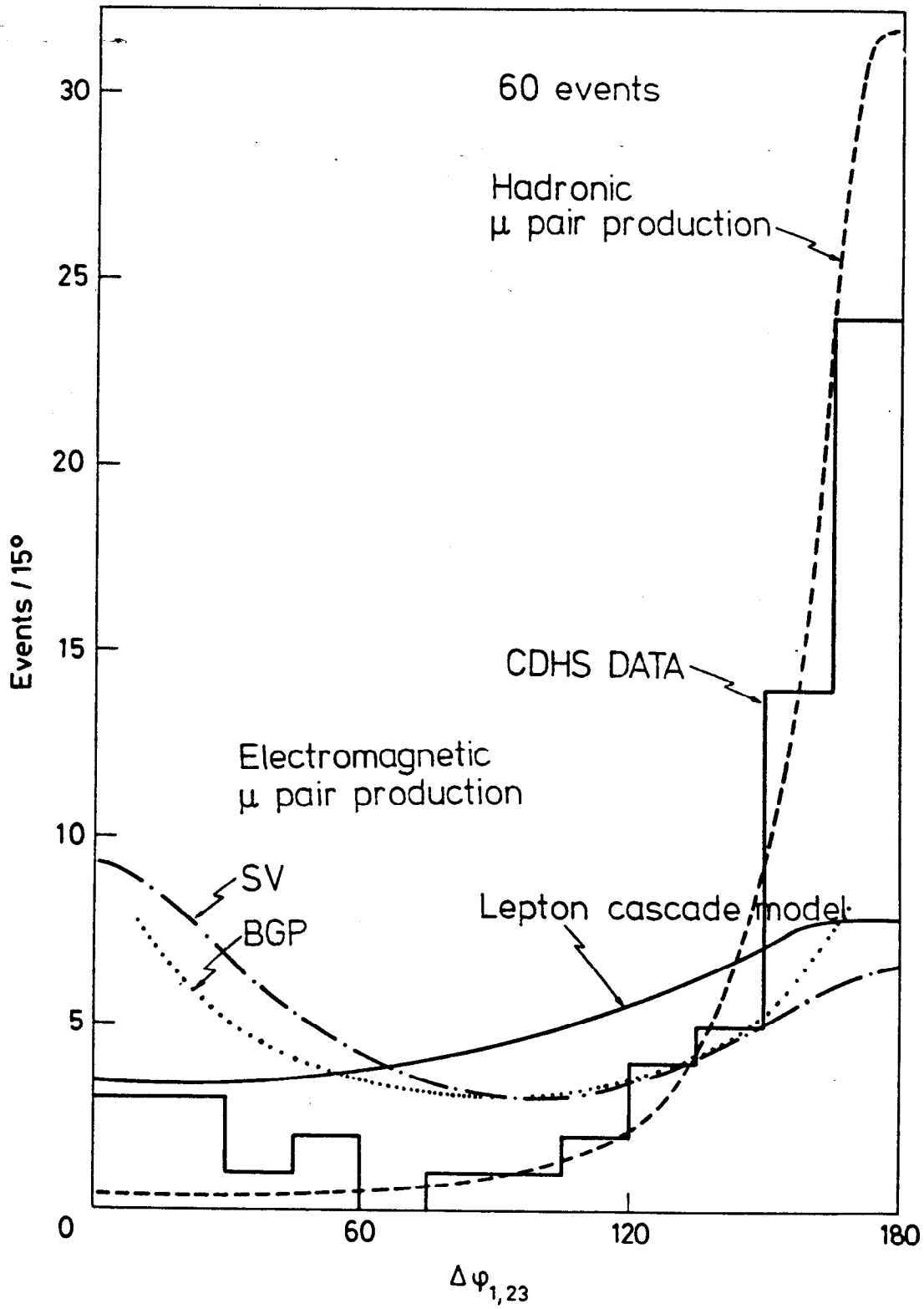

Fig. 30. The trimuon event distribution in $\Delta\phi 1,23$; the angle between the transverse momentum vector of the primary μ^- and the total transverse momentum vector of the $\mu^+\mu^-$ pair. The 0^o peak is ascribed primarily to electromagnetic μ pair production (the process in Fig. 29b), and the 180^o peak is ascribed primarily to hadronic μ pair production (the process in Fig. 29a).

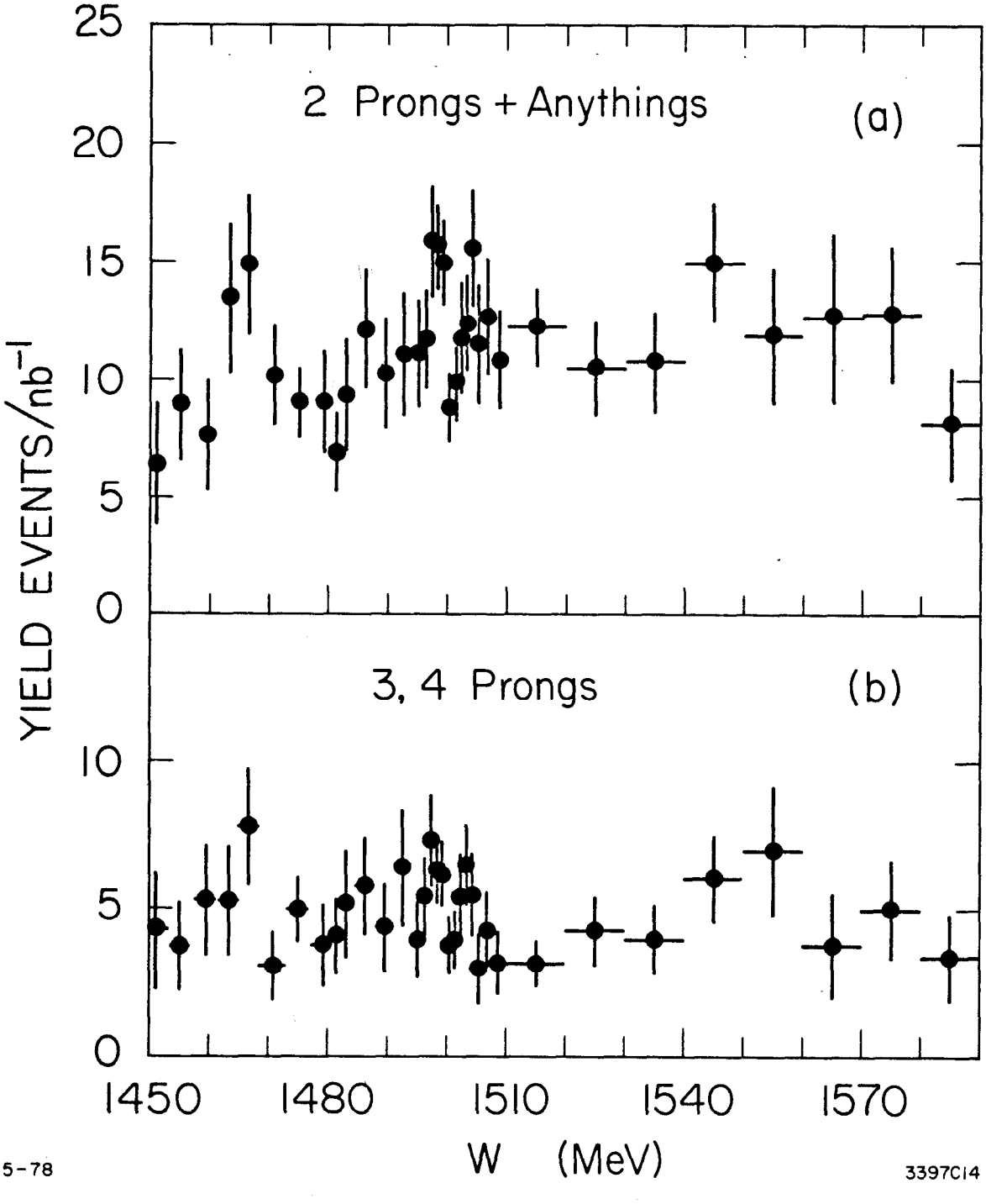

Fig. 31. Structure in various topological cross sections in hadrons produced in e^+e^- annihilation near 1500 MeV. From the $\gamma\gamma$ Group at Frascatti and presented by M. Spinetti, Ref. 70.